TABLE 2. EFFECT OF BDNF ON CERVICAL SPINAL CORD ANTERIOR HORN CELLS 2 WEEKS AFTER ADV INJECTION

		Nissl-positive neurons	*ChAT-positive neurons*	*AChE-positive neurons*
Uninjured AdV-LacZ injected	*n*	1884 ± 154	1678 ± 132	1649 ± 121
	%	100	100	100
Uninjured AdV-BDNF injected	*n*	1256 ± 102†	1165 ± 77†	1056 ± 80†
	%	67 ± 8†	69 ± 9†	64 ± 8†
Injured AdV-LacZ injected	*n*	549 ± 38*†	587 ± 45*†	637 ± 45*†
	%	29 ± 3*†	35 ± 4*†	39 ± 4*†

*$p < 0.05$, compared with AdV-BDNF–injected rats.
†$p < 0.05$, compared with uninjured rats.

AChE-stained neurons survived in AdV-BDNF injected rats, while only 29 ± 3% of Nissl-stained neurons, 35 ± 4% of ChAT-stained neurons, and 39 ± 4% of AChE-stained neurons survived in AdV-LacZ injected rats.

Figure 6 shows photomicrographs of Nissl-, ChAT-, and AChE-stained anterior horn motoneurons at C3 segment at 4 weeks after AdV-BDNF and AdV-LacZ gene transfection. In the AdV-BDNF-treated spinal cord (Fig. 6A–C), the numbers of anterior horn neurons positive for Nissl, ChAT, and AChE staining were higher and clearer than the corresponding neurons of AdV-LacZ-treated rats (Fig. 6D–F).

The numbers of Nissl-, ChAT-, and AChE-stained neurons at each segment of the spinal cord at 2 weeks after gene injection is topographically shown in Figure 7. At the C4 segment of both AdV-BDNF and LacZ-injected rats after spinal cord injury, significant reductions in the numbers of positively stained neurons were observed. Compared with AdV-LacZ injected rats, in the AdV-BDNF-treated spinal cord, the numbers of neurons positive for these stains were significantly higher ($p < 0.05$) at C3–C6, compared to other segments of C1-C2 as well as C7-C8.

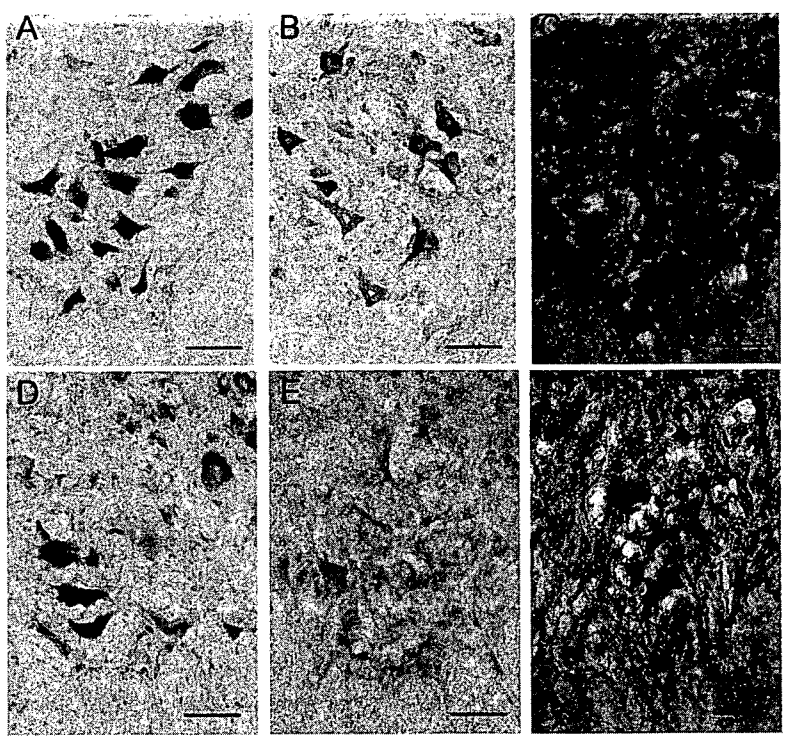

FIG. 6. Photomicrographs showing anterior horn motoneurons at C3 segments of AdV-BDNF injected rats (**A–C**), and AdV-LacZ injected rats (**D–F**) at 4 weeks after spinal cord injury with Nissl staining (A,D), ChAT immunoreactivity (B,E), and AChE activity (C,F). The numbers of motoneurons positive for Nissl, ChAT, and AChE staining were higher in AdV-BDNF injected rats than in AdV-LacZ injected rats. Original magnification, ×200 (A–F).

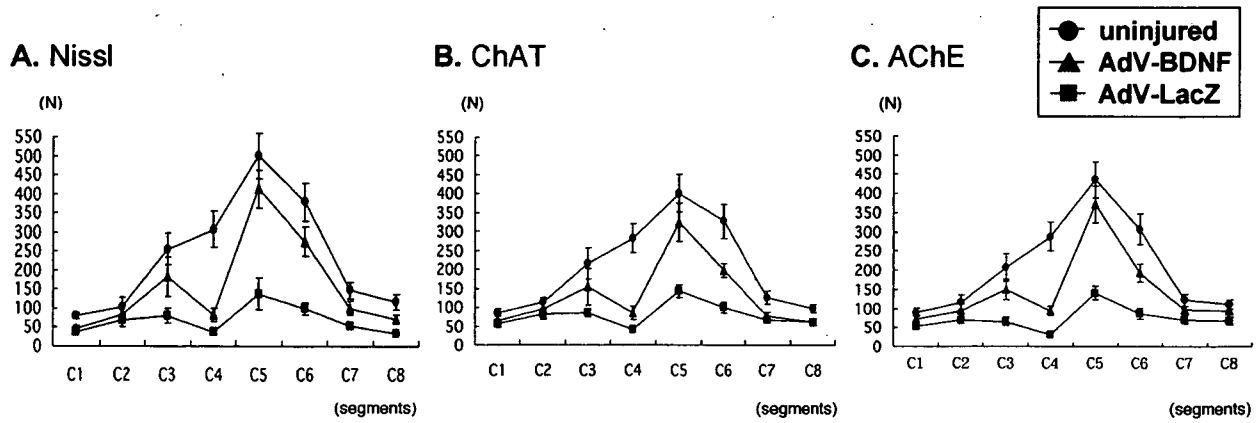

FIG. 7. Topographic changes in the numbers of Nissl-stained (**A**), ChAT-stained (**B**), and AChE-stained (**C**) motoneurons at each cervical segments level at 2 weeks after AdV injection. Note the significantly higher number of survival motoneurons in the adjacent areas, including injured area (C3-C6) than at the distant level (C1-2, C7-8) in injured AdV-BDNF injected rats compared with injured AdV-LacZ injected rats. Data are mean ± SD of 10 rats in each group.

DISCUSSION

The strategies employed to date for the regeneration of injured spinal cord include neutralization of potential growth inhibitory molecules, transplantation of cells or tissue to support axonal outgrowth, and delivery of candidate proteins such as neurotrophic factors (Blesch et al., 2002). Given that numerous steps are required to stimulate axonal growth, guide axons to their targets, and establish new functional synapses, it is essential to combine several methods for improvement of spinal cord and motoneuron function after neuronal injury. A number of approaches have been considered for delivery of neuroprotectants to the spinal cord in order to maintain its normal neural tissue function. It is very important to deliver neurotrophins safely and effectively. Retrograde gene delivery may offer a potential advantage over direct gene administration to the spinal cord in terms of safety, possibility of repeated administration, technical ease of use, and reduction of the inflammatory response in the neural tissue (Yang et al., 1994; Boulis et al., 2003; Nakajima et al., 2005).

Based on experimental work visualizing spinal accessory motoneurons retrogradely by wheat germ agglutinin-horseradish peroxidase labeling method (Kitamura and Sakai, 1982), we established a refined technique to trace motoneurons through the retrograde axonoplasmic transport (Baba et al., 1997; Uchida et al., 1998). Using this technique, we evaluated the efficacy of targeted retrograde gene delivery through the sternomastoid muscle, innervated by spinal accessory nerves, using AdV-BDNF. Exogenous administration of BDNF is expected to promote neuronal cell survival, alleviate neuronal atrophy (Novikova et al., 1996), facilitate axonal regeneration (Kishino et al., 1997; Cai et al., 1999; Liudmila et al., 2002), prevent apoptosis (Giehl et al., 2001), differentiation of neuronal stem cells, and improve motor function (Namiki et al., 2000; Blits et al., 2003; Koda et al., 2004). The mechanism of neuropeptide gene retrograde delivery should be considered from several aspects (Haase et al., 1998); local secretion of protein from AdV-infected muscles, uptake and retrograde axonal transport of AdV in motoneurons, and the secretion of proteins in AdV-infected muscles into the systemic circulation. However, it is difficult to distinguish one of these mechanisms from the others. Previously, we confirmed that LacZ gene expression in the spinal cord was independent from the dosage of exogenously injected AdV-LacZ and, thus, not associated with the systemic circulation. We indicated that AdV-LacZ is transported via retrograde axoplasmic flow through functional axons, or axons neighboring non-functioning ones (Nakajima et al., 2005; Xu et al., 2006).

In the present study, we observed retrograde AdV-BDNF gene expression mainly in the anterior horn motoneurons at least until 4 weeks after spinal cord injury. During spinal cord injury, the few weeks after injury until glial scar formation and/or Wallerian degeneration, are regarded as the turning point for recovery from cell death (Ogawa et al., 2002). Within this period, we showed sufficient preservation of the transduction efficacy of the adenovirus vector. In addition, after AdV-BDNF injection, the surviving anterior horn neurons exhibited significantly increased immunoreactivity to ChAT as well as immunoenzymatic activity to AChE mainly in the adjacent area of the injured spinal cord. In this regard, Nakamura et al. (1996) found a strong correlation between motor function recovery and late high levels of ChAT

activity in the area adjacent to spinal cord injury. Kishino et al. (2003) indicated that neuronal cell survival was less dependent on neurotrophic support than on the expression of cholinergic enzyme activities. Neurotrophic effect at the adjacent area was especially important to the regeneration of the injured spinal cord (Dougherty et al., 2000; Uchida et al., 2003). The present results suggest that AdV-BDNF gene delivery prevented neuronal cell death via increased cholinergic enzyme activity and the sternomastoid muscle was an appropriate target organ for mid to upper cervical spinal cord injury. These findings must be further examined to determine whether AdV-BDNF gene delivery prevented neurotrophin-deficient programmed cell death or other processes at earlier timepoint, and identify the mechanism through which neuronal transmission resulted in neuron preservation. Future studies should help the design of new strategies to prevent neuronal loss after *in vivo* spinal cord injury.

In conclusion, our results suggested that targeted retrograde gene delivery is a potentially suitable approach for the delivery of therapeutic genes important for neuron survival. The method is non-traumatic, effective, selective, with long-lasting gene expression and should suppress the loss of the motoneurons after spinal cord injury.

ACKNOWLEDGMENTS

We are grateful to Drs. Kazunori Yone and Shinji Nakahara, Kagoshima University, for the dedicated technical assistance. This work was supported by Grant-in-Aid (grant nos. 15591571, 16390435, and 17790997) for General Scientific Research from the Ministry of Education, Culture, Sports, Science, and Technology of Japanese Government, and the Japanese Governmental Investigation Committee on Ossification of the Spinal Ligaments (2003–2005).

REFERENCES

BABA, H., MAEZAWA, Y., IMURA, S., KAWAHARA, N., NAKAHASHI, K., and TOMITA, K. (1996). Quantitative analysis of the spinal cord motoneuron under chronic compression: an experimental observation in the mouse. J. Neurol. **243,** 109–116.

BABA, H., MAEZAWA, Y., UCHIDA, K., et al. (1997). Three-dimensional topographic analysis of spinal accessory motoneurons under chronic mechanical compression: an experimental study in the mouse. J. Neurol. **244,** 222–229.

BLACK, P., MARKOWITZ, R.S., COOPER, V., et al. (1986). Models of spinal cord injury: Part 1. Static load technique. Neurosurgery **19,** 752–762.

BLESCH, A., LU, P., and TUSZYNSKI, M.H. (2002). Neurotrophic factors, gene therapy, and neural stem cells for spinal cord repair. Brain Res. Bull. **57,** 83–88.

BLITS, B., OUDEGA, M., BOER, G.J., BARTLETT BUNGE, M., and VERHAAGEN, J. (2003). Adeno-associated viral vector-mediated neurotrophin gene transfer in the injured adult rat spinal cord improves hind-limb function. Neuroscience **118,** 271–281.

BOULIS, N.M., TURNER, D.E., IMPERIALE, M.J., and FELDMAN, E.L. (2002). Neuronal survival following remote adenovirus gene delivery. J. Neurosurg. (Spine) **96,** 212–219.

BOULIS, N.M., WILLMARTH, N.E., SONG, D.K., and FELDMAN, E.L. (2003). Intraneural colchicines inhibition of adenoviral and adeno-associated viral vector remote spinal cord gene delivery. Neurosurgery **52,** 381–387.

CAI, D., SHEN, Y., DE BELLARD, M., TANG, S., and FILBIN, M.T. (1999). Prior exposure to neurotrophins blocks inhibition of axonal regeneration by MAG and myelin via a cAMP-dependent mechanism. Neuron **22,** 89–101.

COLLAZOS, J.E., SOTO, V.M., GUTIERREZ-DAVILA, M., and NIETO-SAMPEDRO, M. (2005). Motoneuron loss associated with chronic locomotion impairments after spinal cord contusion in the rat. J Neurotrauma **22,** 544–558.

DOUGHERTY, K.D., DREYFUS, C.F., and BLACK, I.B. (2000). Brain-derived neurotrophic factor in astrocytes, oligodendrocytes, and microglia/macrophages after spinal cord injury. Neurobiology Dis. **7,** 574–585.

EMBORG, M.E., and KORDOWER, J.H. (2001). Delivery of therapeutic molecules into the CNS. Prog. Brain Res. **128,** 323–332.

GIEHL, K.M., ROHRIG, S., BONATZ, H., et al. (2001). Endogenous brain-derived neurotrophic factor and neurotrophin-3 antagonistically regulate survival of axotomized corticospinal neurons in vivo. J. Neurosci. **21,** 3492–3502.

HAASE, G., PETTMANN, B., VIGNE, E., CASTELNAU-PTAKHINE, L., SCHMALBRUCH, H., and KAHN, A. (1998). Adenovirus-mediated transfer of the neurotrophin-3 gene into skeletal muscle of pmn mice: therapeutic effects and mechanisms of action. J. Neurol. Sci. **160,** S97–S105.

HEDREEN, J.C., BACON, S.J., and PRICE, D.L. (1985). A modified histochemical technique to visualize acetylcholinesterase-containing axons. J. Histochem. Cytochem. **33,** 134–140.

HERMENS, W.T., and VERHAAGEN, J. (1998). Viral vectors, tools for gene transfer in the nervous system. Prog. Neurobiol. **55,** 399–432.

HENDRIKS, W.T., RUITENBERG, M.J., BLITS, B., BOER, G.J., and VERHAAGEN, J. (2004). Viral vector-mediated gene transfer of neurotrophins to promote regeneration of the injured spinal cord. Prog. Brain Res. **146,** 451–476.

KASPAR, B.K., ERICKSON, D., SCHAFFER, D., HINH, L., GAGE, F.H., and PETERSON, D.A. (2002). Targeted retrograde gene delivery for neuronal protection. Mol. Ther. **5,** 50–56.

KEIR, S.D., MITCHELL, W.J., FELDMAN, L.T., and MARTIN, J.R. (1995). Targeting gene expression in spinal cord motor neurons following intramuscular inoculation of an HSV-1 vector. J. Neuro. Virol. **1,** 259–267.

KISHINO, A., ISHIGE, Y., TATSUNO, T., NAKAYAMA, C., and NOGUCHI, H. (1997). BDNF prevent and reverses adult rat motor neuron degeneration and induces axonal outgrowth. Exp. Neurol. **144,** 273–286.

KISHINO, A., and NAKAYAMA, C. (2003). Enhancement of BDNF and activate-ERK immunoreactivity in spinal motor neuron after peripheral administration of BDNF. Brain Res. **964,** 56–66.

KITAMURA, S., and SAKAI, A. (1982). A study on the localization of the sternocleidomastoid and trapezius motoneurons in the rat by means of the HRP method. Anat. Rec. **202,** 527–536.

KODA, M., HASHIMOTO, M., MURAKAMI, M., et al. (2004). Adenovirus vector-mediated in vivo gene transfer of brain-derived neurotrophic factor (BDNF) promotes rubrospinal axonal regeneration and functional recovery after complete transection of the adult rat spinal cord. J. Neurotrauma **21,** 329–337.

KUO, H., INGRAM, D.K., CRYSTAL, R.G., and MASTRANGELI, A. (1995). Retrograde transfer of replication deficient recombinant adenovirus vector in the central nervous system for tracing studies. Brain Res. **705,** 31–38.

LIUDMILA, N., NOVIKOVA, L.N., and KELLERTH, J.O. (2002). Differential effects of neurotrophins on neuronal survival and axonal regeneration after spinal cord injury in adult rats. J. Comp. Neurol. **452,** 255–263.

MANNES, A.J., CAUDLE, R.M., O'CONNELL, B.C., and IADAROLA, M.J. (1998). Adenoviral gene transfer to spinal-cord neurons: intrathecal vs. intraparenchymal administration. Brain Res. **793,** 1–6.

MCDONALD, J.W., LIU, X.Z., QU, Y., et al. (1999). Transplanted embryonic stem cells survive, differentiate and promote recovery in injured rat spinal cord. Nat. Med. **4,** 291–297.

MIYAKE, S., MAKIMURA, M., KANEGAE, Y., et al. (1996). Efficient generation of recombinant adenoviruses using adenovirus DNA-terminal protein complex and a cosmid bearing the full- length virus genome. Proc. Natl. Acad. Sci. USA. **93,** 1320–1324.

NAKAHARA, S., YONE, K., SAKOU, T., et al. (1999). Induction of apoptosis signal regulating kinase 1 (ASK1) after spinal cord injury in rats: possible involvement of ASK1-JNK and -p38 pathways in neuronal apoptosis. J Neuropathol Exp Neurol. **58,** 442–450.

NAKAJIMA, H., UCHIDA, K., KOBAYASHI, S., et al. (2005). Targeted retrograde gene delivery into the injured cervical spinal cord using recombinant adenovirus vector. Neurosci. Lett. **385,** 30–35.

NAKAMURA, M., and BREGMAN, B.S. (2001). Differences in neurotrophic factor gene expression profiles between neonate and adult rat spinal cord after injury. Exp. Neurol. **169,** 407–415.

NAKAMURA, M., FUJIMURA, Y., YATO, Y., WATANABE, M., and YABE, Y. (1996). Changes in choline acetyltransferase activity and distribution following incomplete cervical spinal cord injury in the rat. Neuroscience **75,** 481–494.

NAMIKI, J., KOJIMA, A., and TATOR, C.H. (2000) Effect of brain-derived neurotrophic factor, nerve growth factor, and neurotrophin-3 on functional recovery and regeneration after spinal cord injury in adult rats. J. Neurotrauma **17,** 1219–31.

NOVIKOVA, L.N., NOVIKOV, L.N., and KELLERTH, J.O. (1996). Brain-derived neurotrophic factor reduces necrotic zone and supports neuronal survival after spinal cord hemisection in adult rats. Neurosci. Lett. **220,** 203–206.

OGAWA, Y., SAWAMOTO, K., MIYATA, T., et al. (2002). Transplantation of *in vitro*–expanded fetal neural progenitor cells results in neurogenesis and functional recovery after spinal cord contusion injury in adult rat. J. Neurosci. Res. **69,** 925–933.

PITTENGER, M.F., MACKAY, A.M., BECK, S.C., et al. (1999). Multilineage potential of adult human mesenchymal stem cells. Science **284,** 143–147.

RUITENBERG, M.J., EGGERS, R., BOER, G.J., and VERHAAGEN, J. (2002). Adeno-associated viral vectors as agents for gene delivery: application in disorders and trauma of the central nervous system. Methods **28,** 182–194.

THOMAS, C.E., BIRKETT, D., ANOZIE, I., CASTRO, M.G., and LOWENSTEIN, P.R. (2001). Acute direct adenoviral vector cytotoxicity and chronic, but not acute, inflammatory responses correlate with decreased vector-mediated transgene expression in the brain. Mol. Ther. **3,** 36–46.

UCHIDA, K., BABA, H., MAEZAWA, Y., FURUKAWA, S., FURUSAWA, N., and IMURA, S. (1998). Histological investigation of spinal cord lesions in the spinal hyperostotic mouse (*twy/twy*): morphological changes in anterior horn cells and immunoreactivity to neurotropic factors. J. Neurol. **245,** 781–793.

UCHIDA, K., BABA, H., MAEZAWA, Y., et al. (2003). Increased expression of neurotrophins and their receptors in the mechanically compressed spinal cord of the spinal hyperostotic mouse (twy/twy). Acta Neuropathol. **106,** 29–36.

UCHIDA, K., BABA, H., MAEZAWA, Y., and KUBOTA, C. (2002). Progressive changes in neurofilament proteins and growth-associated protein-43 immunoreactivities at the site of cervical spinal cord compression in spinal hyperostotic mice. Spine **27,** 480–486.

XU, K., UCHIDA, K., NAKAJIMA, H., KOBAYASHI, S., and BABA, H. (2006). Targeted retrograde adenovirus vector carrying brain-derived neurotrophic factor gene transfection prevents loss of mouse (*twy/twy*) anterior horn neurons *in vivo* sustaining mechanical compression. Spine **31,** 1867–1874.

YANG, Y., NUNES, F.A., BERENCSI, K., FURTH, E.E., GONCZOL, E., and WILSON, J.M. (1994). Cellular immunity to viral antigens limits E1-deleted adenoviruses for gene therapy. Proc. Natl. Acad. Sci. USA. **91,** 4407–4411.

Address reprint requests to:
Hideaki Nakajima, M.D.
Division of Orthopaedics and Rehabilitation Medicine
Department of Surgery
University of Fukui Faculty of Medical Sciences
23-3 Matsuokashimoaizuki, Eiheiji-cho, Yoshida-gun
Fukui 910-1193, Japan

E-mail: nhideaki@fmsrsa.fukui-med.ac.jp

SPINE Volume 32, Number 6, pp 627-634

Motor Neuron Involvement in Experimental Lumbar Nerve Root Compression

A Light and Electron Microscopic Study

Shigeru Kobayashi, MD, PhD,* Kenzo Uchida, MD, PhD,* Takafumi Yayama, MD, PhD,* Kenichi Takeno, MD, PhD,* Tsuyoshi Miyazaki, MD,* Seiichiro Shimada, PT,* Masafumi Kubota, PT,* Eiki Nomura, MD, PhD,† Adam Meir, MD,‡ and Hisatoshi Baba, MD, PhD*

Study Design. The aim of this study is to investigate changes in lumbar motor neurons induced by mechanical nerve root compression using an *in vivo* model. This study is to investigate the changes of lumbar motor neuron induced by mechanical nerve root compression using *in vivo* model.

Objectives. The effect of axonal flow disturbance induced by nerve root compression was determined in lumbar motor neuron.

Summary of Background Data. The lumbar motor neuron should not be overlooked when considering the mechanism of weakness, so it is important to understand the morphologic and functional changes that occur in motor neurons of the spinal cord as a result of nerve root compression. However, few studies have looked at changes of neurons within the caused by disturbance of axonal flow, the axon reaction, chromatolysis, and cell death as a result of mechanical compression of the ventral root.

Methods. In mongrel dogs, the seventh lumbar nerve root was compressed for 1 week, or 3 weeks using a clip. Morphologic changes of the motor neurons secondary to the axon reaction were examined by light and electron microscopy.

Results. Light and electron microscopy showed central chromatolysis of motor neurons in the lumbar cord from 1 week after the start of compression. After 3 weeks, some neurons undergoing apoptosis were seen in the ventral horn.

Conclusion. It is important to be aware that, in patients with nerve root compression due to lumbar disc herniation or lumbar canal stenosis, dysfunction is not confined to degeneration at the site of compression but also extends to the motor neurons within the lumbar cord as a result of the axon reaction. Patients with weakness of lower leg should therefore be fully informed of the fact that these symptoms will not resolve immediately after surgery.

From the *Department of Orthopedic Surgery and Rehabilitation Medicine, Fukui University School of Medicine, Fukui, Japan; †Department of Orthopedic Surgery, Kawasaki Municipal Hospital, Kawasaki, Kanagawa, Japan; and ‡Department of Orthopaedic Surgery, Royal Berkshire Hospital, Reading, UK.

Acknowledgment date: May 10, 2006. First revision date: July 13, 2006. Acceptance date: July 13, 2006.

The manuscript submitted does not contain information about medical device(s)/drug(s).

No funds were received in support of this work. No benefits in any form have been or will be received from a commercial party related directly or indirectly to the subject of this manuscript.

Address correspondence and reprint requests to Shigeru Kobayashi, MD, Department of Orthopaedics and Rehabilitation Medicine, Fukui University School of Medicine, Shimoaizuki 23, Matsuoka, Fukui, 910-1193, Japan; E-mail: kshigeru@fmsrsa.fukui-med.ac.jp

Key words: motor neuron, apoptosis, nerve root, compression, radiculopathy, lumbar lesion. **Spine 2007;32: 627-634**

The lumbosacral nerve roots are often involved in disease processes and injuries, such as disc herniation, spinal stenosis, tumor, and vertebral fracture. It is generally considered that the genesis of radiculopathy associated with the pathologic conditions of the spine may result from mechanical compression of the nerve root.[1,2] In experimental studies, many acute[3-15] subacute[16-18] and chronic[19,20] nerve root compression models have been created and have been studied pathologically and electrophysiologically. The results obtained so far suggest that impaired intraradicular blood flow and nerve fiber deformation are implicated in the appearance of radicular symptoms associated with nerve root compression.[21,22] However, few studies have examined the effect of lumbar nerve root compression on axonal reflex caused by compression. It appears that various neurotransmitters produced by the motor neurons in the ventral horn and transported to the axon terminals by axonal flow are implicated in the development of muscle atrophy and motor weakness associated with nerve root compression.

The nerve cell body is essential for the growth and maintenance of the axon. When the axon has injury, the nerve cell body usually undergoes profound alterations in structure, metabolism, and physiologic activity. These changes may be viewed as being specifically appropriate for the repair of the damage, so that the cell body response to axon injury appears to represent a change to a functional state especially conductive to regeneration of the axon. The nerve cell body is known to maintain a high rate of protein synthesis, and there were grounds for the claim that materials that are essential for the survival and efficient functioning of the axon are provided from the cell body by a centrifugal flow of axoplasm.[23,24] Axonal transport conveys neurotransmitters and nerve growth factors and is closely involved in the transmission of information about environmental changes in the axon and target organ. Disruption of axonal flow therefore threatens nerve cell survival and is one cause of neural dysfunction.

Majno and Joris[25] reviewed the histologic development of the cell death concept, with special attention to

the origin of the terms necrosis, coagulation necrosis, autolysis, physiologic cell death, programmed cell death, chromatolysis, karyorrhexis, karyolysis, and cell suicide. They described that Flemming[26] gave a name to the process, chromatolysis, referring to the fact that the broken up nucleus ultimately disappears and apoptosis as observed in 1885 by him, who called it chromatolysis. However, the term chromatolysis was adopted by neuropathologists to mean something entirely different, namely, the apparent breakdown of Nissl substance after transection of the axon. The typical response of the nerve cell body to severance of its axon, first observed by Nissl in 1892,[27] includes an increase in cell body volume, displacement of the nucleus to the periphery and an apparent disappearance of basophilic material from the cytoplasm (chromatolysis). This phenomenon was said axonal reflex, retrograde degeneration, or axonal reaction. Cell death has been classified generally as necrosis or apoptosis, although structural hybrids of neuronal cell death may also occur. Kerr *et al*[28] have reported that there are 2 types of cell death: apoptosis and necrosis. Apoptosis is an active process of cellular self-destruction characterized morphologically by cell shrinkage, cytoplasmic blebbing, chromatin clumping, and formation of apoptotic bodies. The latter are efficiently cleared from the tissue by phagocytes. Necrosis occurs in contiguous groups of cells and is characterized by cell swelling, cell membrane rupture, damaged cytoplasmic organelles, and pyknosis, karyorrhexis or karyolysis of the nuclei. In addition, an inflammatory response is the hallmark of necrosis. However, few studies have looked at changes of neurons within the lumbar cord caused by disturbance of axonal flow and the axon reaction as a result of mechanical compression of the ventral root. The lumbar cord should not be overlooked when considering the mechanism of motor weakness in the legs so it is important to understand the morphologic and functional changes that occur in lumbar motor neurons as a result of nerve root compression. In this study, we used morphologic methods to examine the changes of motor neurons using the nerve root compression model.

■ Materials and Methods

The experiment was carried out under the control of the local animal ethics committee in accordance with the guidelines on animal experiments in our university, Japanese government animal protection and management law, and Japanese government notification on feeding and safekeeping of animals. Twelve adult dogs, weighing 7 to 15 kg, were anesthetized with intramuscular injection of 3 mL of Ketalar (ketamine 50 mg/mL; Warner-Lumbert, Morris Plains, NJ) and ventilated on a respirator under general anesthesia (O_2: 3 mL/min, N_2O: 3 mL/min, halothane: 1.5 mL/min). Animals were maintained at constant physiologic levels during experiment. Each animal was placed in the prone position on a flame. The sixth and seventh lumbar laminae were removed, and the seventh lumbar nerve root was exposed widely on one side. The nerve root was clamped with a clip for microvascular suturing (Kouno Co., Chiba, Japan) at the midpoint between the dural sac and dorsal root ganglion. The 7th nerve root was exposed to compression at 7.5 g force (gf) clipping power.[17,18] In the present study, the strength of the spring clips used for nerve root compression was determined with an Instron-type tensile tester (AGH-2000B, Simazu Co., Kyoto, Japan). Based on the assumption that the strength of the springs follows the law of Young, the weight required to open a clip by 2 mm was determined and 4 types of clips with different compression forces were prepared by adjusting the strength of the spring. The compression force required to open a clip by 2 mm was determined because the transverse diameter of the nerve root is 1.8 ± 0.2 mm.[20] The pressure actually applied to the nerve can be calculated in mm Hg from the following equation: 1033.6 gf/cm^2 = 760 mm Hg. The area (cm^2) of a clip in contact with the nerve is 0.2 cm (width of a clip) × 0.26 cm (longitudinal diameter of L7 nerve root) = 0.052 (cm^2). Therefore, 1 g of force represents about 14.1 mm Hg of pressure. In the previous study, the axonal flow was disturbed by compression at 7.5 gf (about 105.7 mmHg) or higher after 1 week of compression.[29,30] Take *et al*[31] paid attention to the straight leg raising test for diagnosis of lumbar disc herniation, and measured the pressure applied by the herniated mass to the nerve root. When the straight leg raising test was 0°, 30°, 60°, and 90°, the average values of pressure was 32 mm Hg (range, 9–60 mm Hg), 111 mm Hg (20–235 mm Hg), 186 mm Hg (65–367 mm Hg), and 294 mm Hg (130–600 mm Hg), respectively, so the pressure increased with an increasing angle. That is, when compared with the pressure applied to the nerve root measured by Take *et al*[31]in patients with disc herniation, intensification of axonal flow disturbance observed in the present study was assumed to correspond to the pressure applied to the nerve root by SLR of 30° or more.

After awakening from the anesthetic, the animals were maintained for 1 week or 3 weeks and then killed. The animals were fixed by intracardiac perfusion with 4% paraformaldehyde and 1% glutaraldehyde in 0.15 mol/L cacodylate buffer, pH 7.2 at 20 C. After the spinal cord within the 7th lumbar nerve root was harvested, the specimens were examined by either light or electron microscopy. The noncompressed (sham) side was used as a normal control. Each of the specimens was fixed for a further 24 hours in the same fixative. The lumbar cord section was divided into 2 groups. At first, the light microscopy specimens were embedded in paraffin and stained with Klüver-Barrera stain to identify changes of Nissl granules in the neurons. 80 serial 10-μm-thick sections from the rostral end of the 7th lumbar segment of the spinal cord were prepared. Every 10th section was stained using the Klüver-Barrera technique and photomicrographs were taken covering the whole ventral horn in each of the stained sections at a magnification ×200. Motor neurons were counted in ventral horns ipsilateral and contralateral to the L7 nerve root compression and motor neurons showing central chromatolysis were counted.[32,33] Central chromatolysis was identified by round somata with the nucleus in an eccentric position and the Nissl substance displaced toward the margins of the cytoplasm by the pale-staining central area. Neurons were distinguished from glia and inflammatory cells by strict criteria based on perikaryal and nuclear morphology. The criterion for inclusion was any multipolar cell with granular cytoplasmic staining of Klüver-Barrera and nucleus with nucleolus, regardless of size. Cells were excluded if they had a nonneuronal nucleus typical of astrocytes, oligodendrocytes, or microglia. Cell counts were expressed as a ratio of motor neuron number in spinal cord ventral horn ipsilateral and contralateral to the lesion. Statistical analyses of motor

Figure 1. Light micrographs in the ventral root at the site of compression (**A**) and central to the site of compression (**B**) after 3 weeks. Toluidine blue stain; scale bars = 100 μm in A and B.

neuron numbers per postlesion time point were performed using a nonparametric test (Wilcoxon's rank sum test) with SPSS statistical software, version 11.0J (SPSS Inc., Chicago, IL).

The other sections were rinsed in 0.05 mol/L Tris-HCl buffer, postfixed at room temperature for 3 hours in 2% OsO_4 in 0.1 mol/L sodium cacodylate buffer, impregnated with 2% uranyl acetate, dehydrated in graded ethanols, and embedded in epoxy resin. For light microscopy, 1- to 3-μm-thick toluidine blue-stained sections were used. For electron microscopy, ultrathin sections contrasted with uranyl acetate and lead citrate were examined a under JSM2000 electron microscope (JEOL Ltd., Tokyo, Japan).

■ Results

After 1 and 3 weeks, nerve fiber degeneration was observed not only at the site of compression but also in the peripheral zone of a compressed ventral root (Figure 1A). No Wallerian degeneration was evident in the ventral root central to this site even at 3 weeks after compression (Figure 1B). After 1 and 3 weeks, histologic examination of the uncompressed site revealed nerve fiber deformation but no appreciable Wallerian degeneration.

Examination of the neurons in contralateral ventral horn by light microscopy showed that the nucleus was round, light-colored, and centrally located; the nucleolus was distinct; and the striped Nissl granules in the cytoplasm were intensely stained by Klüver-Barrera stain (Figures 2A, 3A). Light microscopy showed, however, that central chromatolysis of ipsilateral motor neurons was evident at 1 week postlesion (Figure 2B, 4A). In the neurons with chromatolysis, the nucleus had moved to the periphery and the number of Nissl bodies in the central cytoplasm was decreased. These changes became more marked and the number of neurons with central chromatolysis was increased significantly after 3 weeks compression ($P < 0.01$) (Figure 2C; Table 1). The Nissl

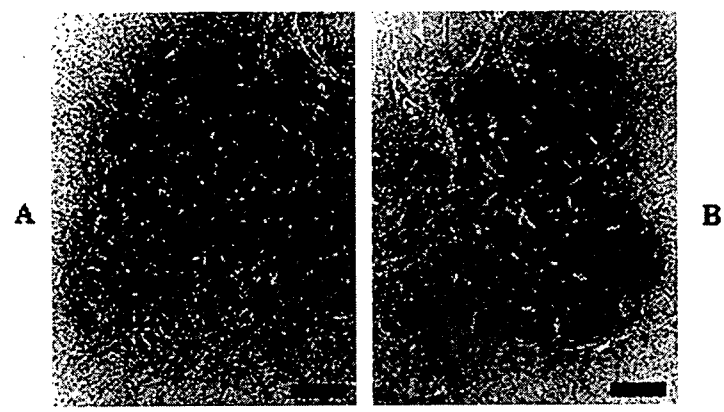

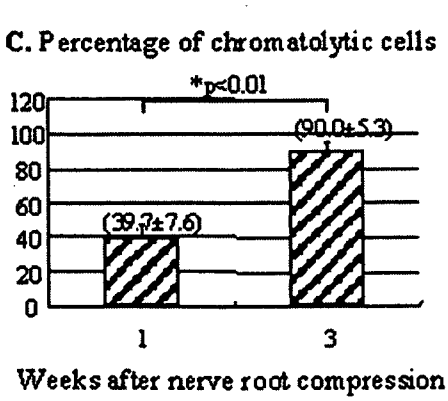

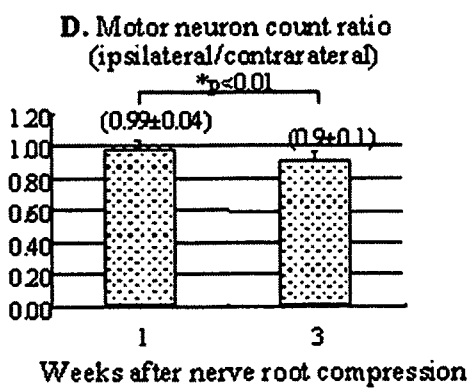

Figure 2. Changes of motor neurons in the ventral horn after nerve root compression. **A** and **B**, Constructed light micrographs of ventral horn obtained after ventral root compression for 1 week. A, Sham side. B, Compression side. Central chromatolysis (arrow) was seen in the ventral horn in comparison of the neurons of sham side. Klüver-Barrera stain. Scale bars = 250 μm in A and B. **C**, The percentage of chromatolytic cells increased significantly with time by root compression. *$P < 0.01$ *versus* the value of 1 week compression group. **D**, Number of remaining motor neurons in lumbar spinal cord ventral horn at different times after nerve root compression. Motor neuron count ratio (ipsilateral/contralateral side) decreased significantly with time by root compression. *$P < 0.01$ *versus* the value of 1 week compression group.

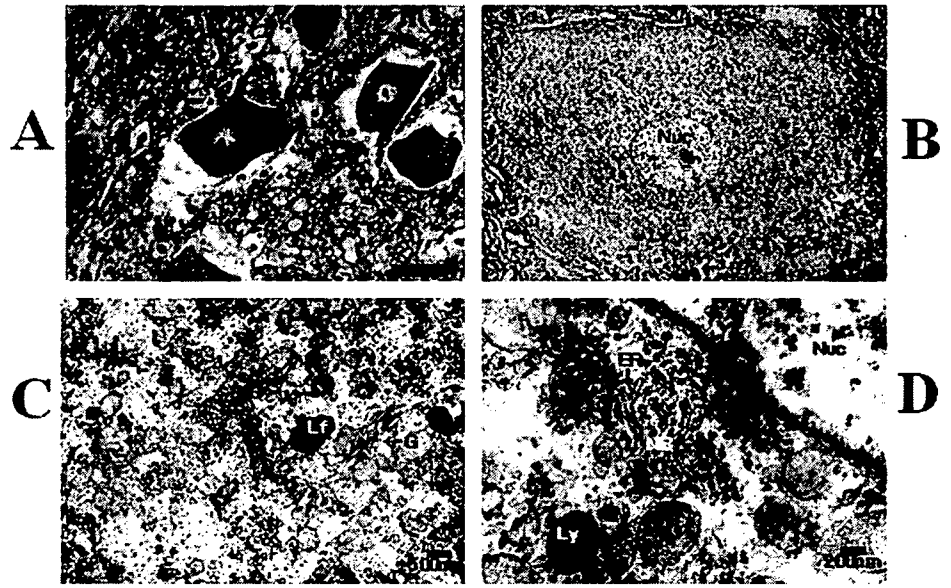

Figure 3. Light (**A**) and electron (**B–D**) micrographs of contralateral motor neurons. A, Control motor neuron. Klüver-Barrera stain, Scale bars = 50 μm. B, In this motor neuron, the nucleus was centrally located; fine-grained chromatin was widely scattered throughout the nucleus. C, The Golgi apparatus and Nissl bodies. D, Cluster-like Nissl bodies are made up of rough endoplasmic reticulum and ribosomes. Nuclear pore have not appeared in the nuclear membrane. (Original magnifications: B, ×1200; C, ×10,000; D, ×30,000). ER, rough surfaced endoplasmic reticulum; G, Golgi apparatus; Lf, lipofuscin granule; Ly, lysosome; Mit, mitochondria; NB, Nissl body; Nuc, nucleus; r, free ribosome.

bodies resembled fine powder at the cell periphery and were only present in small numbers (Figure 5A). The transverse section of spinal cord at L7 shows the apparent loss of motor neurons in ventral horn ipsilateral to the nerve root compression at 1 and 3 weeks postlesion (Table 1). Motor neuron count ratio (ipsilateral/contralateral side) decreased significantly with time by root compression (Figure 2D).

On electron microscopy, the nucleus of contralateral side was centrally located; fine-grained chromatin was widely scattered throughout the nucleus; and Nissl bodies, mitochondria, Golgi apparatus, lysosomes, and neurofilaments were present in the cytoplasm. The clusters of Nissl bodies distributed throughout the cytoplasm were made up of free ribosomes not attached to the endoplasmic reticulum as well as rough endoplasmic reticulum with ribosomes attached. Nuclear clefts in normal neurons typically are devoid of organelles (Figure 3B–D). Light and electron microscopy showed no appreciable changes of the contralateral motor neurons after compression for 3 weeks. After 1-week compression, however, electron microscopy showed that the nucleus of ipsilateral side started to move to the periphery (Figure 4B–D). In the cytoplasm, dissolution of the perinuclear Nissl bodies was evident, and many mitochondria showed elongation and vacuolation. There was also an increase of nuclear pores. After 3 weeks of compression, these changes became more marked, there was loss of rough endoplasmic reticulum and mitochondria from the central cytoplasm, and these structures were replaced by many vesicles, vacuoles, and filaments (Figure 5B–D). Some neurons undergoing apoptosis were seen in the ventral horn (Figure 6A). The neurons and nuclei were reduced in size and chromatin condensation was seen in the nuclei. Electron microscopy revealed apoptosis character-

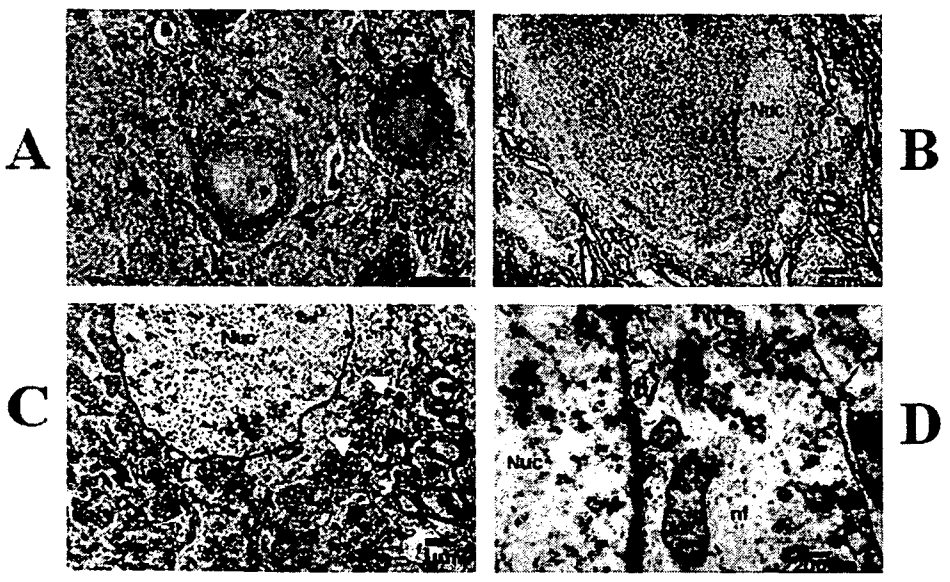

Figure 4. Light (**A**) and electron (**B–D**) micrographs of motor neurons after ventral root compression for 1 week. A, The nucleus has moved to the periphery of the cell, loss of perinuclear Nissl bodies is evident, and central chromatolysis had started. Klüver-Barrera stain. Scale bars = 50 μm. B, In this motor neuron, the nucleus had moved toward the cell periphery. C, Loss of perinuclear Nissl bodies is evident (white arrow). D, Dissolution of the Nissl bodies has started and scattered ribosomes are present around the nucleus. The cisterns of rough surfaced endoplasmic reticulum are enlarged. Many pores have also appeared in the nuclear membrane. The border of the cell. Nissl bodies are still present, but some mitochondria show vacuolation. (Original magnifications: B, ×1200; C, ×6000; D, ×30,000). ER, rough surfaced endoplasmic reticulum; Mit, mitochondria; NB, Nissl body; nf, neurofilament; Nuc, nucleus.

Table 1. Changes of Motor Neurons in the Lumbar Ventral Horn at Different Times After the 7th Nerve Root Compression

	Contralateral Side			Ipsilateral Side			
Subject No.	No. of Neurons/8 Sections	No. of Chromatolytic Neurons/8 Sections	% of Chromatolytic Cells	No. of Neurons/8 Sections	No. of Chromatolytic Neurons/8 Sections	% of Chromatolytic Cells	Motor Neuron Count Ratio (ipsilateral/ contralateral)
1 week after nerve root compression							
1	125	0	0	123	56	45.5	0.98
2	126	0	0	135	62	45.9	1.07
3	123	0	0	121	38	31.4	0.98
4	123	1	0.8	121	56	46.3	0.98
5	107	0	0	102	30	29.4	0.95
6	121	0	0	116	46	39.7	0.96
Average	120.8	0.2	0.1	119.7	48.0	39.7	0.99
SEM	7.0	0.4	0.3	10.7	12.3	7.6	0.04
3 weeks after nerve root compression							
7	127	0	0	111	99	89.2	0.87
8	127	0	0	110	99	90.0	0.87
9	130	1	0.8	122	112	91.8	0.94
10	111	0	0	92	87	94.6	0.83
11	124	1	0.8	120	96	80.0	0.97
12	121	0	0	118	111	94.1	0.98
Average	123.3	0.3	0.3	112.2*	100.7	90.0	0.9
SEM	6.8	0.5	0.4	11.0	9.5	5.3	0.1

SEM, standard error of the mean. Motor neurons were counted in the level of 7th lumbar spinal cord. Klüver-Barrera stain transverse section of spinal cord at L7 level shows the apparent loss of motor neurons and the increase of chromatolytic cells in the ventral horn ipsilateral to the nerve root compression at 3 weeks postlesion.
*Significant difference ($P < 0.05$) from contralateral side.

ized by condensation of the nuclei and chromatin condensation, and destruction of the organelles in the cytoplasm. The cytoplasm contains numerous small vacuoles, some of which are degenerating mitochondria (Figure 6B).

■ Discussion

The characteristic axonal transport system of neurons, which comprises anterograde and retrograde flow, plays an important role in the movement of neurotransmitters and neurotrophic factors as well as in the transmission of information relating to environmental changes in the axon itself and the target organ. Disturbance of axonal flow therefore threatens the survival of neurons and appears to be one cause of neurologic dysfunction. In this study, compression of the peripheral branches of motor neurons in the nerve root led to impairment of axonal flow and central chromatolysis in the neurons of the ventral horn, where the peripheral branches of these neurons originated. Chromatolysis is

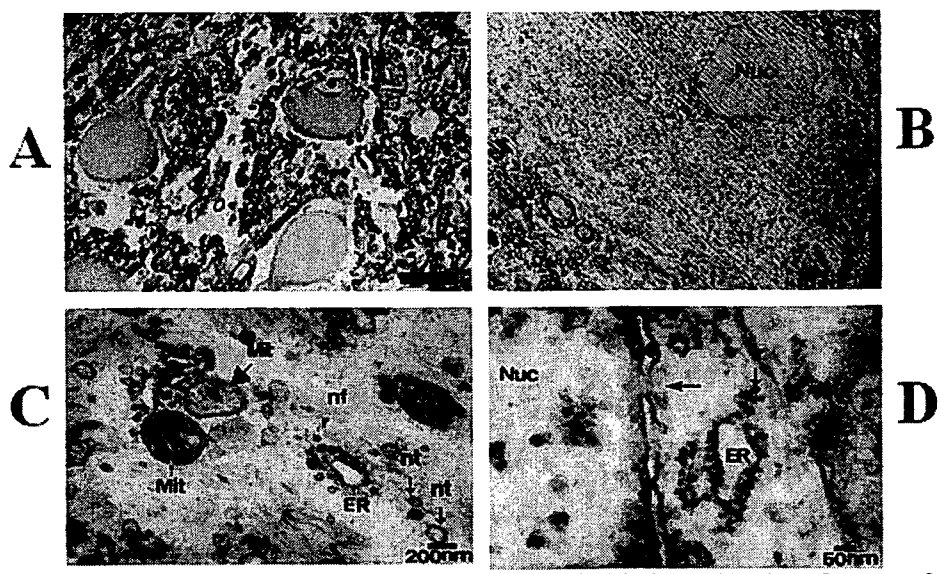

Figure 5. Light (**A**) and electron (**B–D**) micrographs of motor neurons after ventral root compression for 3 weeks. A, There is an increase of neurons exhibiting obvious central chromatolysis. Klüver-Barrera stain. Scale bars = 50 μm. B, In this motor neuron, the nucleus had moved to the periphery. C, The border of the cell. Loss of Nissl bodies and vacuolation of many mitochondria are evident. Ribosomes are scattered. There is a decrease of rough endoplasmic reticulum, ribosomes, and mitochondria, as well as an increase of neurofilaments and neurotubules. D, Enlargement of the perinuclear region. Vesiculated cisternae have few ribosomes on membrane. Ribosomes are free and on polysomal formations. Nuclear pore have also appeared in the nuclear membrane. (Original magnifications: B, ×1200; C, ×30,000; D, ×100,000). ER, rough surfaced endoplasmic reticulum; Mit, mitochondria; nf, neurofilament; nt, neurotubule; Nuc, nucleus; r, free ribosome.

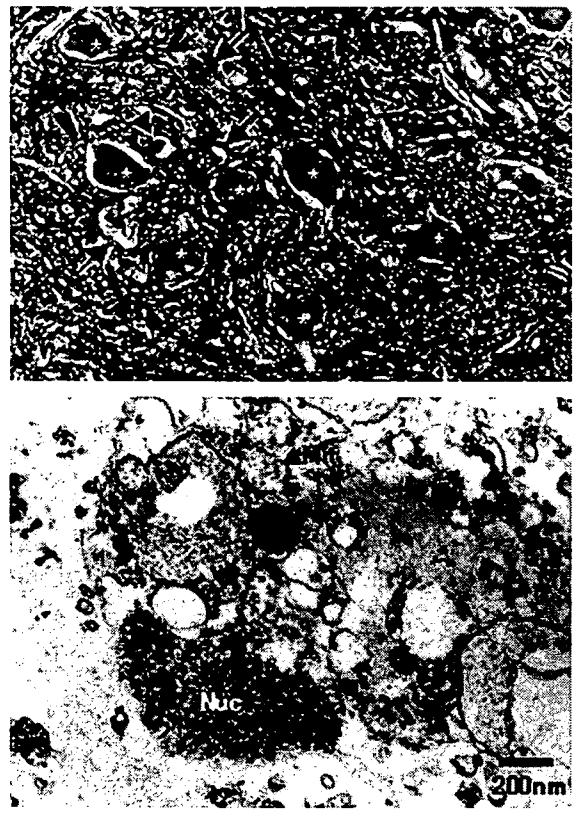

Figure 6. Light and transmission electron micrographs of apoptotic motor neurons. **A**, Light microscopy showed central chromatolysis (*) and apoptosis (arrow) of motor neurons after ventral root compression for 3 weeks. The apoptotic neurons were reduced in size and chromatin condensation was seen in the nuclei. Klüver-Barrera stain. Scale bars = 50 μm. **B**, Ventral root compression-induced degeneration of motor neuron is apoptosis. Electron microscopy revealed apoptosis characterized by condensation of the nuclei and chromatin condensation, and destruction of the organelles in the cytoplasm. The cytoplasm contains numerous small vacuoles, some of which are degenerating mitochondria. (Original magnification, ×30,000).

a reactive change of neuronal perikarya to axonal injury. The classic histologic features, namely, the peripheral margination of Nissl substance, nuclear displacement, and nucleolar enlargement, are manifestations of the cell's attempt to regenerate the injured axon. Neurodegeneration following axonotomy and target deprivation has been studied for many years in animal models,[24,34–36] and the likely role of neurotrophin deprivation in this neurodegeneration is well recognized.[37–41] The dependence of these changes on the type and location of the lesion indicates that the chromatolytic reaction is mediated by retrograde signals from the site of injury.[24,35,42–49] This reaction reflects an alteration in the arrangement and concentration of RNA-containing material in the cell, leading to changes in protein synthesis of importance for axonal regeneration. However, there have been few studies into the effect of mechanical lumbar nerve root compression on motor neuron in the ventral horn.

Many researchers suggested that, in cells that are extremely active in protein synthesis, the nucleus may be elaborately convoluted and this is interpreted as a device for increasing the surface area of the nucleus to meet the exceptional demand for interaction of nucleus and cytoplasm.[24,37–41] The axotomized neurons react to provide the increased metabolic activity needed for regeneration of the axon and show the increased RNA and protein synthesis.[24] The irregular nuclear membrane and presence of numerous nuclear pores may be associated with an increase in RNA and protein synthesis induced by increased synthesis of ribonucleoprotein and its subsequent transfer to the cytoplasm. In this study, there was an increase of nuclear pores after nerve root compression for 1 week. A decrease in the number of ribosomes attached to the endoplasmic reticulum and an increase of free ribosomes were also observed in these neurons due to fragmentation of the rough endoplasmic reticulum making up the Nissl bodies. A decrease in the number of ribosomes attached to the endoplasmic reticulum and an increase of free ribosomes were also observed in these neurons due to fragmentation of the rough endoplasmic reticulum making up the Nissl bodies. Ribosomes are ribonucleoproteins (RNP) that are made up of RNA and protein. Free ribosomes produce proteins that are constituents of the cell itself, while the rough endoplasmic reticulum synthesizes proteins for export by secretion and other means. It has been demonstrated that central chromatolysis inhibits neurotransmitter synthesis and other neuronal functions, but stimulates the metabolism of structural proteins such as those of the cytoskeleton and the synthesis of nerve growth factor that are required to maintain axonal integrity or for axonal regeneration, as well as production of lipids for membrane (Figure 7). It seems likely that sustained mechanical compression of the nerve root could result in irreversible damage to the motor neurons. The morphologic changes that we observed in lumbar motor neurons after mechanical compression of the nerve root therefore reflect the metabolic response to axonal degeneration and regeneration. If the disturbance of axonal flow caused by compression and the resulting central chromatolysis are mild, the neuron can recover fully after compression is relieved. However, it seems likely that sustained mechanical compression of the nerve root could result in irreversible damage to the neurons of the ventral horn, such as apoptosis. Chromatolysis does not necessarily foreshadow neuronal cell death after axotomy,[46] although specific signals during chromatolysis may be required to initiate apoptosis after axotomy. Chromatolysis following axotomy can be blocked or delayed when RNA synthesis is inhibited with actinomycin D,[47] thereby implicating activation of gene transcription and protein synthesis in the molecular signaling for this structural response. In the context of axotomy-induced neuronal apoptosis, this finding is important because some type of programmed cell death can be prevented by inhibitors of RNA and protein synthesis.[50] Thus, a regenerative-degenerative response continuum may exist after axotomy that begins as chromatolysis and evolves into either repair and survival of neurons or apoptosis of neurons (Figure 7C). Al-Abdulla *et al*[51] described that the retrograde degeneration of geniculocortical projection neurons that occurs after visual cortex ablation in the

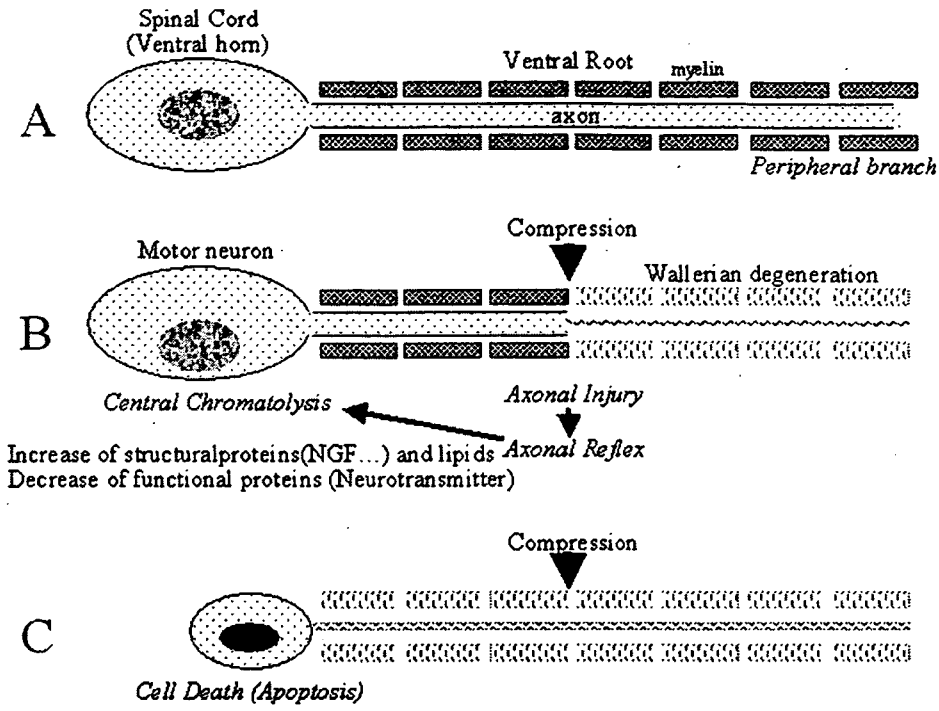

Figure 7. Functional changes of motor neurons after nerve root compression. **A**, Normal. **B**, Central chromatolysis. **C**, Cell death (apoptosis).

adult brain is apoptosis, based on morphologic criteria. They concluded the morphologic changes that occur during this process progress from chromatolysis through consecutive stages associated with apoptosis. Martin *et al*[52] noted that motor neuron death after sciatic nerve avulsion resembles apoptosis. Nissl-stained sections of spinal cord were used to construct a staging shame for the structural progression of motor neuron death. Over 14 days, neurons pass through chromatolytic stages and then undergo apoptosis. They described that mitochondria may participate in the signaling of injured, chromatolytic motor neurons to enter apoptosis, possibly by releasing cytochrome c or by generating excessive reactive oxygen species. An important contribution of the present study is the discovery that nerve root compression-induced, retrograde degeneration of motor neurons in the ventral horn structurally resembles apoptosis. Apoptotic neuron had a shrunken perikaryon that contained small vacuoles and numerous mitochondria within a dense cytoplasmic matrix. We observed that this retrograde neurodegeneration evolves from classic chromatolysis to apoptosis over 21 days.

As clinicians, we often come across patients with cauda equina and nerve root compression due to lumbar disc herniation or lumbar canal stenosis who continue to experience muscle atrophy and weakness long after surgical decompression of the nerve root, particularly patients with a long history of weakness in the lower extremities before surgery. It is therefore important to be aware that, in patients with mechanical nerve root compression, dysfunction is not confined to degeneration at the site of compression but also extends to the motor neurons within the ventral horn as a result of the axon reaction. Patients with a long history of weakness in the lower extremities should therefore be fully informed of the fact that these symptoms will not resolve immediately after surgery.

■ Key Points

- Morphologic changes of the motor neurons induced by nerve root compression were examined by light and electron microscopy.
- Light and electron microscopy showed central chromatolysis and apoptosis of motor neurons in the lumbar cord after nerve root compression.
- The lumbar motor neuron should not be overlooked when considering the mechanism of weakness, so it is important to understand the morphologic changes that occur in motor neurons of the cord as a result of nerve root compression.

Acknowledgment

The authors thank Mr. Naruo Yamashita who provided expert help with the photography as well as Mrs. Kyoko Shimokawa, Ms. Mika Osaki, and Ms.Yukiko Horiuchi for their dedicated assistance in this study.

References

1. Kobayashi S, Shizu N, Suzuki Y, et al. Changes of nerve root motion and intraradicular blood flow during an intraoperative SLR test. *Spine* 2003;28: 1427–34.
2. Kobayashi S, Suzuki Y, Asai T, et al. Changes of nerve root motion and intraradicular blood flow during an intraoperative femoral nerve stretch test. *J Neurosurg (Spine 3)* 2003;28:298–305.
3. Delamarter RB, Bohlman HH, Dodge LD, et al. Experimental lumbar spinal stenosis: analysis of the cortical evoked potential, microvasculature, and histopathology. *J Bone Joint Surg Am* 1990;72:110–20.
4. Gelfan S, Tarlov IM. Physiology of spinal cord, nerve root, and peripheral nerve compression. *Am J Physiol* 1956;185:217–29.
5. Kobayashi S, Yoshizawa H, Hachiya Y, et al. 1993 Volvo Award Winner in

Basic Science Studies. Vasogenic edema induced by compression injury to the spinal nerve root: distribution of intravenously injected protein tracers and gadolinium-enhanced magnetic resonance imaging. *Spine* 1993;18:1410–24.
6. Kobayashi S, Yoshizawa H, Nakai S. Neurophysiological changes of the nerve root induced by mechanical compression. In: Takahashi HE, ed. *Mechanical Loading of Bones and Joints*. Tokyo: Spronger-Verlag 1999:245–58.
7. Kobayashi S, Yoshizawa H, Nakai S. Experimental study on the dynamics of lumbosacral nerve root circulation. *Spine* 2000;25:298–305.
8. Kobayashi S, Yoshizawa H. Effect of mechanical compression on the vascular permeability of the dorsal root ganglion. *J Orthop Res* 2002;20:730–9.
9. Kobayashi S, Baba H, Uchida K, et al. Imaging of intraneural edema by using gadolinium-enhanced MR imaging: experimental compression injury. *AJNR Am J Neuroradiol* 2005;26:973–980.
10. Kobayashi S, Baba H, Uchida K, et al. Effect of mechanical compression on the lumbar nerve root: localization and changes of intraradicular inflammatory cytokines, nitric oxide, and cyclooxygenase. *Spine* 2005;30:1699–705.
11. Kobayashi S, Uchida K, Takeno K, et al. Imaging of the cauda equina edema in lumbar canal stenosis using Gadolinium-enhanced MR imaging: experimental constriction injury. *AJNR Am J Neuroradiol* 2006;27:346–53.
12. Olmarker K, Rydevik B, Holm S. Edema formation in spinal nerve roots induced by experimental, graded compression: an experimental study on the pig cauda equina with special reference to differences in effects between rapid and slow onset of compression. *Spine* 1989;14:569–73.
13. Rydevik B, Pedowitz RA, Hargens AR, et al. Effects of acute, graded compression on spinal nerve root function and structure: an experimental study of the pig cauda equina. *Spine* 1991;16:487–93.
14. Yoshizawa H, Kobayashi S, Kubota K. Effect of compression on intraradicular blood flow in dogs. *Spine* 1989;14:1220–5.
15. Yoshizawa H, Kobayashi S, Hachiya Y. Blood supply of nerve roots and dorsal root ganglia. *Orthop Clin North Am* 1991;22:195–211.
16. Cornefjoid M, Sato K, Olmarker K, et al. A model for chronic nerve root compression studies: presentation of a porcine model for controlled, slow-onset compression with analysis of anatomic aspects, compression onset rate, and morphologic and neurophysiologic effects. *Spine* 1997;22:946–57.
17. Kobayashi S, Yoshizawa H, Yamada S. Pathology of lumbar nerve root compression: Part 1. Intraradicular inflammatory changes induced by mechanical compression. *J Orthop Res* 2004;22:170–9.
18. Kobayashi S, Yoshizawa H, Yamada S. Pathology of lumbar nerve root compression: Part 2. Morphological and immunohistochemical changes of dorsal root ganglion. *J Orthop Res* 2004;22:180–8.
19. Iwamoto H, Kuwahara H, Matsuda H, et al. Production of chronic compression of the cauda equina in rats for use in studies of lumbar spinal canal stenosis. *Spine* 1995;20:2750–7.
20. Yoshizawa H, Kobayashi S, Morita T. Chronic nerve root compression: pathophysiologic mechanism of nerve root dysfunction. *Spine* 1995;20:397–407.
21. Hasue M. Pain and the nerve root: an interdisciplinary approach. *Spine* 1993;18:2053–8.
22. Rydevik B, Brown MD, Lundborg G. Pathoanatomy and pathophysiology of nerve root compression. *Spine* 1984;9:7–15.
23. Cragg BG. What is the signal for chromatolysis? *Brain Res* 1970;23:1–21.
24. Lieberman AR. The axon reaction: a review of the principal features of perikaryal responses to axon injury. *Int Rev Neurobiol* 1971;14:49–124.
25. Majno G, Joris I. Apoptosis, oncosis, and necrosis: an overview of cell death. *Am J Pathol* 1995;146:3–15.
26. Flemming W. Über die Bildung von Richtungsfiguren in Säugethiereiern beim Untergang Graaf'scher Follikel. *Arch Anat EntwGesch* 1885;221–44.
27. Nissl F. Über die Veränderungen der Ganglienzellen am Facialiskern des Kaninchens nach Ausrei Bung der Nerven. *Allg Z Psychiat Grenz* 1892;48:197–8.
28. Kerr JFR, Harmon BV. Definition and incidence of apoptosis: an historical perspective. In: Tomei LD, Cope FO, eds. *Apoptosis: The Molecular Basis of Cell Death*. Cold Spring Harbor, NY: Cold Spring Harbor Laboratory Press, 1991:5–29.
29. Kobayashi S, Kokubo Y, Uchida K, et al. Effect of lumbar nerve root compression on primary sensory neurons and their central branches: changes in the nociceptive neuropeptides substance P and somatostatin. *Spine* 2005;30:276–82.
30. Kobayashi S, Sasaki S, Shimada S, et al. Changes of calcitonin gene-related peptide in primarily sensory neuron and their central branch after nerve root compression of the dog. *Arch Phys Med Rehabil* 2005;86:527–33.
31. Take O, Matuzaki H, Hoshino M, et al. Pathology and pressure of the nerve root at the herniated site during straight leg raising test: lumbar disc herniation. *J Jpn Orthop Assoc* 1989;63(suppl):1008.
32. Sobue G, Terao S, Kachi T, et al. Somatic motor effects in multiple system atrophy with autonomic failure: a clinico-pathological study. *J Neurol Sci* 1992;112:113–25.
33. Terao S, Sobue G, Hashizume Y, et al. Disease-specific patterns of neuronal loss in the spinal ventral horn in amyotrophic lateral sclerosis, multiple system atrophy and X-linked recessive bulbospinal neuronopathy, with special reference to the loss of small neuron in the intermediate zone. *J Neurol* 1994;241:196–203.
34. LaVelle A, LaVelle FW. The nucleolar apparatus and neuronal reactivity in injury during development. *J Exp Zool* 1958;137:285–315.
35. Ramon y Cajal S. *Degeneration and Regeneration of the Nervous System*. New York: Oxford University Press, 1928:769–70.
36. Torvik A. Central chromatolysis and the axon reaction: a reappraisal. *Neuropathol Appl Neurobiol* 1976;2:423–32.
37. Hefti F. Nerve growth factor promotes survival of septal cholinergic neurons after fimbrial transection. *J Neurosci* 1986;6:2155–62.
38. Kromer LF. Nerve growth factor treatment after brain injury prevents neuronal death. *Science* 1987;235:214–6.
39. Oppenheim RW, Qin-Wei Y, Prevette D, et al. Brain-derived neurotrophic factor rescues developing avian motoneurons from cell death. *Nature* 1992;360:755–7.
40. Stockli KA, Lottspeich F, Sendtner M, et al. Molecular cloning, expression and regional distribution of rat ciliary neurotrophic factor. *Nature* 1989;342:920–3.
41. Yan Q, Elliott J, Snider WD. Brain-derived neurotrophic factor rescues spinal motor neurons from axotomy-induced cell death. *Nature* 1992;360:753–5.
42. Fry FJ, Cowan WN. A study of retrograde cell degeneration in the lateral mammillary nucleus of the cat, with special reference to the role of axonal branching in the preservation of the cell. *J Comp Neurol* 1972;144:1–24.
43. Hall ME, Wilson DL, Stone GC. Changes in synthesis of specific proteins following axonotomy: detection with two-dimensional gel electrophoresis. *J Neurobiol* 1978;9:353–66.
44. Hughs JT. Central chromatolysis. In: *Pathology of the Spinal Cord*. London: Lloyd-Luke, 1978:3–5.
45. Kirkpatrick JB. Chromatolysis in the hypoglossal nucleus of the rat: an electron microscopic analysis. *J Comp Neurol* 1968;132:189–212.
46. Price DL, Porter KR. The response of ventral horn neurons to axonal transection. *J Cell Biol* 1972;53:24–37.
47. Torvik A, Heding A. Effect of actinomycin D on retrograde nerve cell reaction: further observations. *Acta Neuropathol* 1969;14:62–71.
48. Torvik A, Skjorten F. Electron microscopic observations on nerve cell regeneration and degeneration after axon lesions. *Acta Neuropathol (Berl)* 1971;17:248–64.
49. Watson WE. Observations on the nucleolar and total cell body nucleic acid of injured nerve cells. *J Physiol (Lond)* 1968;196:655–76.
50. Sen S. Programmed cell death: concept, mechanism and control. *Biol Rev* 1992;67:287–319.
51. Al-Abdulla NA, Portera-Cailliau C, Martin LJ. Occipital cortex ablation in adult rat causes retrograde neuronal death in the lateral geniculate nucleus that resembles apoptosis. *Neuroscience* 1998;86:191–209.
52. Martin LJ, Kaiser A, Price AC. Motor neuron degeneration after sciatic nerve avulsion in adult rat evolves with oxidative stress and is apoptosis. *J Neurobiol* 1999;40:185–201.

SPINE Volume 32, Number 19, pp E551–E556

How Does the Ossification Area of the Posterior Longitudinal Ligament Thicken Following Cervical Laminoplasty?

Takeshi Hori, MD, Yoshiharu Kawaguchi, MD, and Tomoatsu Kimura, MD

Study Design. Retrospective case series.

Objective. To investigate the progression of the thickness of the ossification area over time following cervical laminoplasty.

Summary of Background Data. Cervical laminoplasty has become the standard technique for the treatment of patients with myelopathy due to ossification of the posterior longitudinal ligament (OPLL). However, OPLL is a progressive disease, and an increase in the area of ossification following laminoplasty affects the surgical results. To date, complete analysis of the thickness of OPLL progression has not been undertaken because changes in the ossification thickness are minor compared with those of the longitudinal axis.

Methods. Fifty-five patients who were available for serial radiographs more than 5 years after cervical laminoplasty were included. The extent of ossification thickness was assessed using lateral radiographs of the cervical spine and computer software. The neurologic evaluation was graded using the Japanese Orthopedic Association score (JOA score). The associations between the progression of OPLL and the clinical and radiologic data were analyzed. We also evaluated the progression of the thickness of the ossification area over time following surgery.

Results. Twelve patients (21.8%) had progression in the OPLL thickness. Progression was marked in younger patients with the mixed or continuous types of OPLL. C3 involvement was also common in the patients with the OPLL progression. The progression of OPLL thickness was not directly related to the score-based recovery rate. The progression of OPLL was frequently observed at C2, C3, and C4 levels. Progression in OPLL thickness was detected in 42.1% of C2 ossifications, 13.3% of C3, 11.9% of C4, 4.1% of C5, 5.5% of C6, and 6.6% of C7.

Conclusion. Young patients with continuous or mixed-type OPLL and C3 involvement of ossification had a risk for progression in OPLL thickness following surgery. As the increased thickness of ossified lesions directly causes the narrowing of the spinal canal, it is important to pay attention to these risk factors and the increase in ossification before and after cervical laminoplasty in the surgical treatment of patients with OPLL.

From the Department of Orthopaedic Surgery, University of Toyama, Toyama, Japan.
Acknowledgment date: November 1, 2006. First revision date: February 1, 2007. Acceptance date: April 13, 2007.
The manuscript submitted does not contain information about medical device(s)/drug(s).
No funds were received in support of this work. No benefits in any form have been or will be received from a commercial party related directly or indirectly to the subject of this manuscript.
Address correspondence and reprint requests to Yoshiharu Kawaguchi, MD, Department of Orthopaedic Surgery, University of Toyama, Faculty of Medicine, 2630, Sugitani, Toyama 930-0194, Japan; E-mail: zenji@med.u-toyama.ac.jp

Key words: cervical laminoplasty, ossification of the posterior longitudinal ligament, long-term follow-up, thickening of ossification. **Spine 2007;32:E551–E556**

Ossification of the posterior longitudinal ligament (OPLL) is characterized by replacement of the ligamentous tissue by ectopic new bone formation. OPLL has been recognized as one of the causes of cervical myelopathy.[1] In our institute, *en bloc* cervical laminoplasty has been indicated in most patients with cervical myelopathy due to OPLL since 1981.[2] Excellent results following laminoplasty have been reported in the treatment of patients with OPLL.[3,4] But OPLL is a progressive disease, and it has been reported that an increased area of ossification affects the surgical results in the long-term follow-up after laminoplasty.[5,6] In the analysis of the progression of the OPLL longitudinal axis, it has been confirmed that the progression of OPLL is common in younger patients with continuous or mixed types of ossification.[7] The pattern of OPLL progression can be classified into 3 groups. Group 1, patients in their 40s with continuous or mixed-type OPLL, an initial slow and then rapid progression pattern; Group 2, patients aged over 50 years old with continuous or mixed-type OPLL, an initial rapid and then slow progression pattern; and Group 3, patients with segmental-type OPLL and no or a slight progression pattern. These findings are very important for the management of patients with OPLL after surgery. We especially have to pay a lot of attention for the neurologic changes at the patients in Group 1 and Group 2 with long-term follow-up after surgery because they might have a risk of developing myelopathy due to the progression of OPLL. However, to date, the progression in OPLL thickness has not been thoroughly analyzed, due to the more minor changes in ossification thickness compared with those of the longitudinal axis. The progression of the thickness of the ossified lesion is more important as it directly leads to the narrowing of the spinal canal.[6] The purpose of the present study was to investigate the progression of the thickness of the ossification area over time following cervical laminoplasty.

Materials and Methods

A total of 122 patients with OPLL underwent *en bloc* cervical laminoplasty for the treatment of cervical myelopathy at our hospital between 1981 and 1997. The details of the procedure for cervical laminoplasty have been described in previous reports.[2,3] Radiographs of the cervical spine were taken every 3 months within 1 year after surgery, and then once a year there-

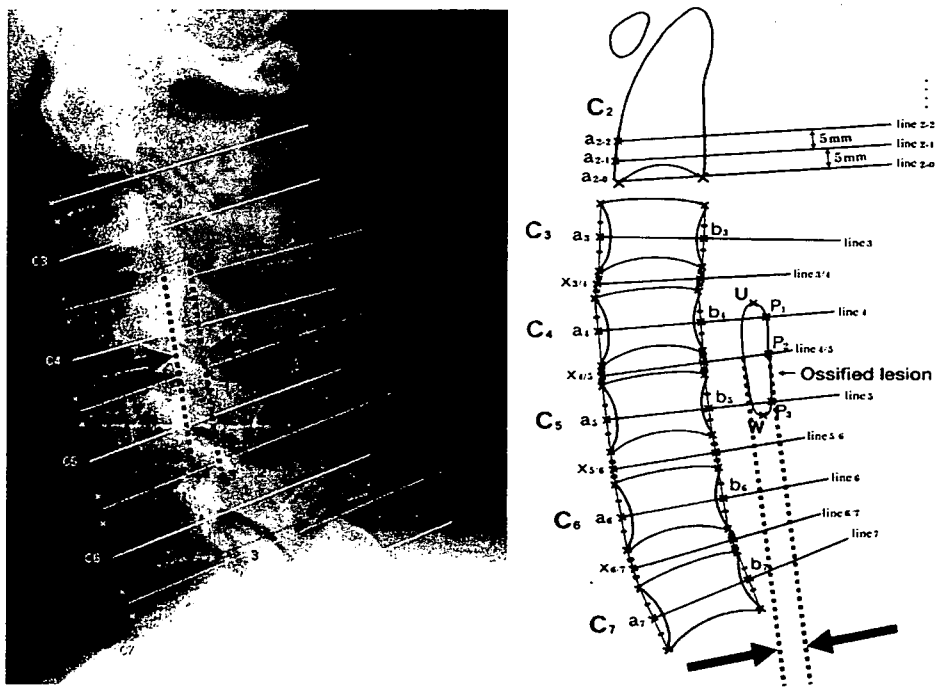

Figure 1. A computer software, which measures the progression of OPLL (OPLL Draw Version 2J; Array Corp., Tokyo). The tool was developed for the measurement of the longitudinal axis and the sagittal thickness of the ossification area in OPLL. Radiographic and schematic drawing shows the reference points and lines drawn by the tool. The details of this measurement method were previously described by Chiba *et al.*[8,9] An observer selects 2 inferior corners of the axis body for C2 and 4 corners of each vertebral body from C3–C7 by clicking on the image displayed on a computer screen with a mouse pointer. The software automatically draws reference points and lines. P, posterior margin; U, upper end; W, lower end. Dotted lines and lines with arrows indicate the measurement of thickness of the ossified lesion.

after. Fifty-five patients who had available serial radiographs of more than 5 years were included in this study. There were 38 men and 17 women with an average age of 56.7 years old (range, 42–75 years) at the time of the operation.

Radiographs of the cervical spine were taken before the operation and at 6 months, 1 year, 3 years, 5 years, and 10 years after the operation in our institute. Lateral radiographs were made with a constant distance from the tube to the film and from the spine to the film. The radiographs were scanned and preserved in a personal computer. The extent of ossification thickness was assessed at each level of the cervical spine on lateral radiographs using a software which measures the progression of OPLL (OPLL Draw Version 2J; Array Corp., Tokyo, Japan) (Figure 1).[7–9] The alignment of the cervical spine was also evaluated. The alignment was measured in the lateral view in the neutral position as lordosis and kyphosis based on the angle between the lines passing through the lower margin of the C2 vertebral body and C6 or C7. The lordotic angle was represented as a positive value and the kyphotic angle, a negative value. Ossification types were classified as continuous, segmental, mixed, and localized types according to the criteria proposed by the Investigation Committee on the Ossification of Spinal Ligaments of the Japanese Ministry of Public Health and Welfare (Figure 2).[10]

As previously described, the progression of OPLL in the longitudinal axis was defined as an increased ossification of >2 mm at the point of final follow-up. Progression of OPLL in thickness was also defined as an increased ossification of >2 mm at the final follow-up (the progression group). The following items were compared between the progression group and the nonprogression group: age of patients at the time of operation, sex, the type of OPLL, the progression of OPLL in longitudinal axis, the existence of barsony, which is the ossification of ligamentum nuchae, the existence of ossification of the anterior longitudinal ligament, the existence of ossification at C3, alignment of the cervical spine, and the existence of overlapping OPLL at the same level.[11]

Neurologic function was graded according to the scale devised by the Japanese Orthopedic Association (JOA).[12] The rate of recovery was calculated with use of the following formula: [postoperative score − preoperative score] × 100/[17 (score for full recovery) − preoperative score]. The JOA score and score based rate of recovery were compared between the progression group and the nonprogression group. Further-

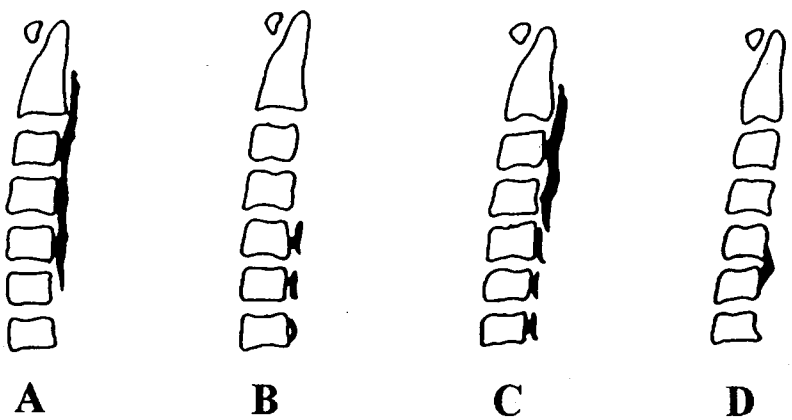

Figure 2. Classification of ossification of the posterior longitudinal ligament by the Investigation Committee on the Ossification of the Spinal Ligaments, Japanese Ministry of Public Health and Welfare. **A**, Continuous type. **B**, Segmental type. **C**, Mixed type. **D**, Localized type.

more, we assessed the correlation between the progression width of OPLL in thickness and JOA score based rate of recovery in progression group.

We also analyzed the progression in the thickness of ossification after surgery. The change in the length of the progression of the ossification area from before operation to 6 months after operation, from 6 months to 1 year, from 1 year to 3 years, from 3 years to 5 years, and from 5 years to 10 years was measured. Then, we analyzed the speed of the OPLL thickness progression per year.

Statistical Analysis. Statistical analyses were performed using Stat View (SAS Inc., Cary, NC). Data were presented as the mean value and the standard deviation. A *t* test was used for statistical analysis of the difference between the age of the progression group and the age of the nonprogression group. The same statistical method was used for analysis of the effect of preoperative cervical alignment on the progression of OPLL thickness. A χ^2 test was used for analysis of the difference in the progression of OPLL among the types of OPLL and the other clinical features. A Pearson's correlation coefficient was used for analysis of the coefficient of correlation between the progression of OPLL in thickness and JOA score based rate of recovery in progression group. A *P* value of <0.05 was considered to be significant.

■ Results

The continuous type of ossification was observed in 13 patients, the segmental type in 17, the mixed type in 23, and the localized type in 2 patients before surgery. At the time of the final follow-up, the type of ossification had changed from mixed to continuous in 9 patients, from segmental to continuous in 1, and from segmental to mixed in 1. Twelve (21.8%) of the 55 patients had progression in OPLL in thickness following laminoplasty (Table 1). The average increase in thickness was 3.5 mm (2–8.5 mm) in patients that progressed.

Comparison of the Clinical Features Between the Groups With and Without the Progression of Ossification Thickness

The average age of the patients with the progression of OPLL thickness was 51.8 ± 8.4 years (n = 12), whereas the average age of the patients without thickness progression was 58.1 ± 9.2 years (n = 43). The average age of the progression group was significantly younger than that of the nonprogression group ($P = 0.04$). Progression was common in patients with the mixed or continuous types, whereas it was never seen in those with the segmental type. The difference was significant ($P = 0.038$). The patients who showed the OPLL progression in the longitudinal axis also had a risk factor for progression of OPLL thickness ($P = 0.02$).

Table 1. Comparison of the Preoperative OPLL Type Between the Progression Group and the Nonprogression Group

	Progression Group (N = 12) (preoperative)	Nonprogression Group (N = 43) (preoperative)
Continuous	5	8
Segmental	0	23
Mixed	7	10
Localized	0	2

$P = 0.0382$.

Table 2. Comparison of the Clinical Features Between the Progression Group and the Nonprogression Group

	Progression Group (N = 12)	Nonprogression Group (N = 43)	*P*
Age (yr)	51.8 ± 8.4	58.07 ± 9.2	0.04
Cervical alignment (°)	11.6 ± 10.1	8.8 ± 13.2	0.52
Sex (male/female)	10/2	28/15	0.20
Progression in longitudinal axis (±)	12/0	29/14	0.02
Barsony (±)	9/3	34/9	0.77
OALL (±)	7/5	22/21	0.97
Presence of C3 OPLL (±)	11/1	19/24	0.001
Overlapped OPLL (±)	3/9	11/32	0.97
Recovery rate based on JOA score (%)	60.5 ± 39.9	61.9 ± 36.2	0.91

There was no consistent association between the progression of OPLL and sex, the existence of barsony, which is the ossification in the ligamentum nuchae, the existence of ossification of the anterior longitudinal ligament, alignment of the cervical spine, and the existence of overlapping OPLL. However, the OPLL progression was marked in the patients with ossification at C3, compared with the patients without ossification at that level ($P = 0.001$) (Table 2).

The JOA score improved rapidly within 1 year and continued to improve for up to 5 years after surgery in both the progression group and nonprogression group. The mean score in progression group increased from 8.0 points before surgery to 13.0 points, and the recovery rate was 60.5% at final follow up. The mean score in the nonprogression group increased from 8.6 to 13.7, and the recovery rate was 61.9%. The progression of OPLL thickness was not directly related to the score based recovery rate (Table 2).

The coefficient of correlation between the progression of OPLL in thickness and JOA score based rate of recovery was also assessed in progression group. A Pearson's correlation coefficient was 0.063. Therefore, there was no significant correlation between the progression of OPLL and recovery rate.

Vertebral Level of Increased Ossification Thickness

Figure 3 shows the vertebral level of increased thickness of OPLL in 12 patients. Progression in OPLL thickness was detected in 22 vertebral levels. Eight cases revealed the progression in C2, 4 in C3, 5 in C4, 2 in C5, 2 in C6, and 1 in C7. Progression in OPLL thickness was detected in 42.1% at C2, 13.3% at C3, 11.9% at C4, 4.1% at C5, 5.5% at C6, and 6.6% at C7. The progression of ossification thickness was marked in C2, C3, and C4 levels.

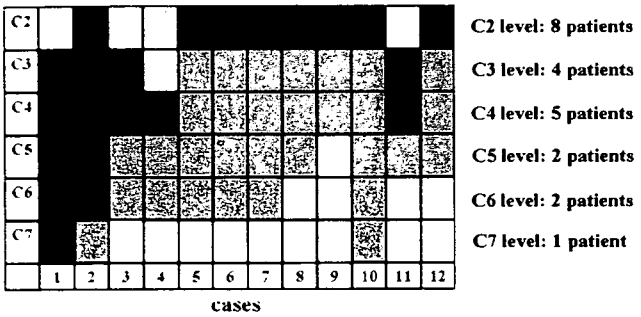

Figure 3. Vertebral level of increased ossification of OPLL thickness. Black partitions show the vertebral levels of ossification, which show an increased OPLL thickness. The gray partitions indicate the vertebral levels of ossification, which did not increase in thickness.

How Does the Thickness of the Ossification Area Progress After Cervical Laminoplasty?

The progression of OPLL thickness was found in 2 patients at 6 months after surgery, 9 patients at 1 year, 15 patients at 3 years, and 22 patients at 5 years after laminoplasty (Figure 4). The average increase was 1.0 ± 1.3 mm at 1 year and 3.3 ± 1.1 mm at 5 years after surgery. The average progression ratio of the patients in their 40s was 0.55 mm/yr (n = 11), whereas the average progression ratio of the patients aged over 50 was 0.6 mm/yr (n = 11). There was no significant difference between the average progression ratios and the age at surgery. However, 1 patient (44 years old at operation) showed 8.5 mm of the OPLL thickness progression at C2 10 years after surgery. Fortunately, she did not have any clinical symptoms as a result of the progression. On the other hand, the OPLL progression stopped by 3 years after surgery in 2 patients more than 65 years of age.

Illustrative Cases

Case 1. This 48-year-old man with mixed-type OPLL had progressive myelopathy (Figure 5A). The patient underwent C3–C7 laminoplasty. The OPLL thickness at C3–C4 had increased by 3 mm from the operation to 5 years after the operation (Figure 5B). Then, the progression of ossification thickness continued until 11 years after the operation (Figure 5C).

■ Discussion

As for the evaluation of OPLL progression, our method using a lateral radiograph of the cervical spine and computer-assisted software to measure OPLL has been confirmed in several studies.[7–9,13] To date, we regard this method to be the best means of measurement of the OPLL progression because the method is very simple and precise. Intraobserver and interobserver reliability was reported to be high in a multicenter study.[9]

In the current study, progression of OPLL thickness was found in 21% of the patients with a greater than 5-year follow-up after cervical laminoplasty. The average increase of ossification thickness was 3.5 mm. Such an increase in the ossified lesion area directly affects the narrowing of the spinal canal. Thus, the patients with OPLL thickness progression have a risk of relapse of spinal canal narrowing. This study showed that the young patients with continuous or mixed type and C3 involvement of ossification frequently showed OPLL thickness progression after surgery. This is in agreement with the result of the risk factor for OPLL progression in the longitudinal axis.[7] Therefore, we must pay attention to these preoperative characteristics of ossification with respect to the ossification progression of both the thickness and longitudinal axis in the long-term follow-up after laminoplasty. In contrast, OPLL thickness progression was never seen in the patients with the segmental type of OPLL. Our previous study also revealed that the segmental type of OPLL rarely had progression in the longitudinal axis.[7] These facts might indicate that the pathology of ossification is different between the segmen-

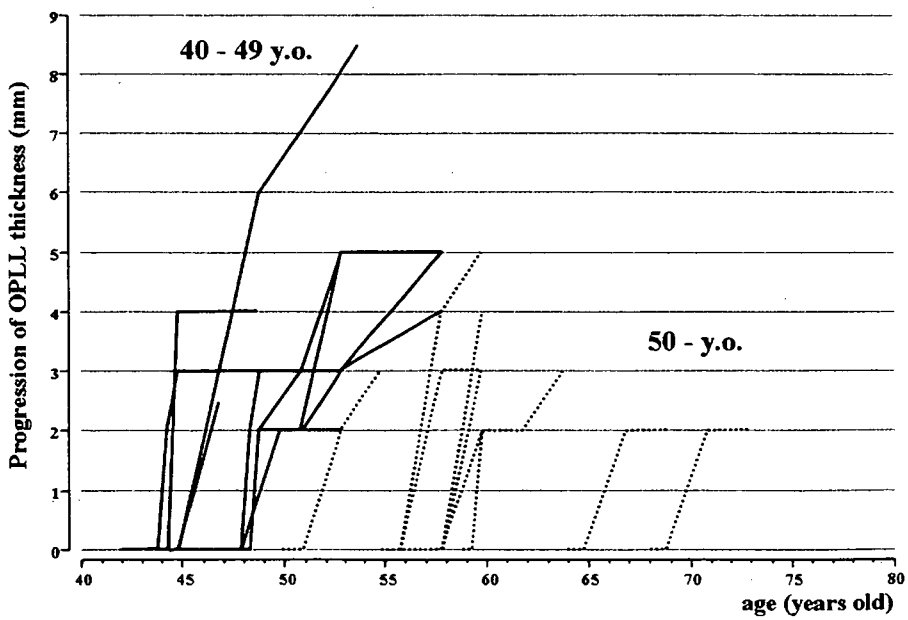

Figure 4. The association between the progression of OPLL thickness and the age of the patients. The solid lines indicate the progression of OPLL thickness in the patients in their 40s, and the dotted lines indicate that in the patients aged over 50s.

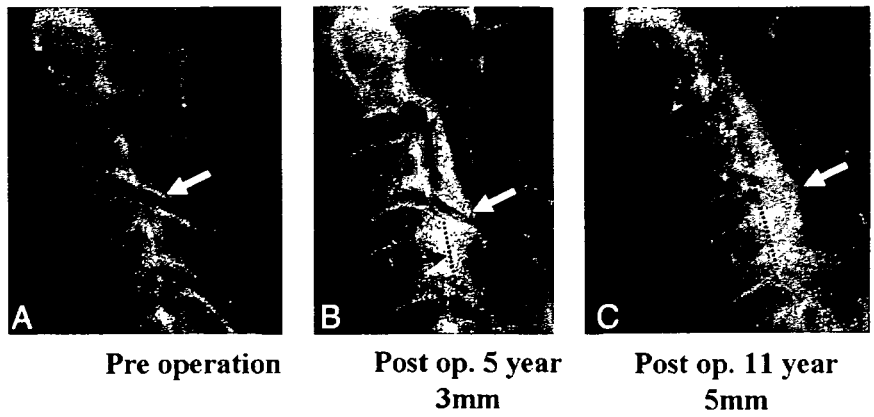

Figure 5. This 48-year-old man with mixed-type OPLL had progressive myelopathy (**A**). The patient underwent C3–C7 laminoplasty. The progression of OPLL thickness had increased by 3 mm during the time from the operation to 5 years after the operation (**B**). Then, the progression in thickness continued to 11 years after the operation (**C**). White arrows indicate the ossified lesions on radiograph. Dotted lines and lines with arrows show the measurement of the thickness of the ossified lesions.

tal type and the other types (mixed and the continuous types).

The current study revealed that the progression of ossification thickness was marked at the upper cervical levels rather than at the lower levels. The incidence of the progression was frequent at C2, C3, and C4. The progression of OPLL in the longitudinal axis was also remarkable toward the cranial portion. In contrast, a previous study suggested that ossification of OPLL was most frequently observed at C5 and C4.[5] These facts might indicate that OPLL develops at C5 or C4 in the initial stage and then the ossification area later spreads in both thickness and longitudinal axis at the upper cervical levels. The speed of the progression of ossification thickness in patients in their 40s was the same as that of the patients over 50 years old. However, the OPLL progression stopped in the patients over 65 years old. Our previous study showed that the speed of the progression of ossification thickness was faster in the patients in their 40s, whereas that of the patients over 60 years old was slow.[7] These facts suggest that the OPLL ossification progression weakens in older patients.

In the current study, we analyzed the progression of OPLL in patients who had *en bloc* laminoplasty. Our previous study revealed that 3 (7%) of 45 patients had neurologic deterioration due to the progression of OPLL after cervical laminoplasty.[6] It has also been reported that 2% to 35% of the patients had neurologic deterioration due to an increase in the thickness of OPLL following laminoplasty.[4,14–16] The cervical laminoplasty procedure has several merits such as expanding the spinal canal, securing spinal stability, and sparing the protective function of the spinal cord, compared with that of laminectomy.[3] Laminoplasty is now a standard technique for the treatment of patients with cervical compressive myelopathy. However, preserved laminae might become a compressive factor by the progression of OPLL in the long-term after laminoplasty.

The results of the current study showed no significant difference in the JOA score based recovery rate at final follow-up between the progression group and nonprogression group. In the same way, there was no significant correlation between the progression of OPLL and recovery rate in the progression group. These results indicate that the progression of OPLL thickness is not related to the deterioration in neurologic function. Matsunaga *et al* reported that the risk factors associated with the evolution of myelopathy include greater than 60% OPLL-induced stenotic compromise of the cervical canal and increased range of motion of the cervical spine. In the current study, the average increase in OPLL thickness was 3.5 mm. Therefore, if once the enlargement of spinal canal was performed by cervical laminoplasty, the occupation ratio of the OPLL rarely exceeds 60% of spinal canal. This is one reason that the progression of OPLL thickness was not directly related to the deterioration in neurologic function.

However, some patients developed a neurologic deterioration in both the progression and nonprogression groups. In our current study, we assessed the cervical alignment but did not check the range of motion of cervical spine. As Matsunaga *et al*[17] stated, the dynamic factor of cervical spine might be important for the development of neurologic deterioration after cervical laminoplasty.

■ Conclusion

A total of 21.8% of the patients had progression of OPLL thickness after cervical laminoplasty in the long-term follow-up. The progression of OPLL was marked in C2, C3, and C4. The young patients with continuous or mixed-type OPLL and C3 involvement of ossification were at risk for progression of OPLL thickness after surgery. The progression of OPLL thickness was rarely related to the deterioration in neurologic function. It is important to pay a lot of attention to the complaints of patients, and not to overlook the sign of the neurologic deterioration.

■ Key Points

- The progression of the thickness of the ossified lesion was analyzed using a computer software.
- A total of 21.8% of the patients had progression of OPLL thickness after cervical laminoplasty in the long-term follow-up.

- The young patients with continuous or mixed-type OPLL and C3 involvement of ossification were at risk for progression of OPLL thickness after surgery.
- The progression of OPLL was marked in C2, C3, and C4 levels.

References

1. Tsukimoto H. On an autopsied case of compression myelopathy with a callus formation in the cervical spinal canal [in Japanese]. *Nihon Geka Hokan.* 1960;29:1003–7.
2. Itoh T, Tsuji H. Technical improvements and results of laminoplasty for compressive myelopathy in the cervical spine. *Spine* 1985;10:729–36.
3. Kawaguchi Y, Kanamori M, Ishihara H, et al. Minimum 10-year followup after en bloc cervical laminoplasty. *Clin Orthop* 2003;411:129–39.
4. Iwasaki M, Kawaguchi Y, Kimura T, et al. Long-term results of expansive laminoplasty for ossification of the posterior longitudinal ligament of the cervical spine: more than 10 years follow up. *J Neurosurg* 2002;96:180–9.
5. Hirabayashi K, Miyakawa J, Satomi K, et al. Operative results and postoperative progression of ossification among patients with ossification of cervical posterior longitudinal ligament. *Spine* 1981;6:354–64.
6. Kawaguchi Y, Kanamori M, Ishihara H, et al. Progression of ossification of the posterior longitudinal ligament following en bloc cervical laminoplasty. *J Bone Joint Surg Am* 2001;83:1798–802.
7. Hori T, Kawaguchi Y, Kimura T. How does the ossification area of the posterior longitudinal ligament progress after cervical laminoplasty? *Spine* 2006;31:2807–12.
8. Chiba K, Kato Y, Tsuzuki N, et al. Computer-assisted measurement of the size of ossification in patients with ossification of the posterior longitudinal ligament in the cervical spine. *J Orthop Sci* 2005;10:451–6.
9. Chiba K, Yamamoto I, Hirabayashi H, et al. Multicenter study investigating the postoperative progression of ossification of the posterior longitudinal ligament in the cervical spine: a new computer-assisted measurement. *J Neurosurg Spine* 2005;3:17–23.
10. Investigation Committee on OPLL of the Japanese Ministry of Public Health and Welfare. The ossification of the posterior longitudinal ligament of the spine (OPLL). *J Jpn Orthop Assoc* 1981;55:425–40.
11. Zeidman SM, Ducker TB. Evaluation of patients with cervical spine lesion. In Clark CR (ed.). *The Cervical Spine.* Third ed. Philadelphia: Lippincott Raven Publishers; 1998:p143–61.
12. Kato Y, Tsuzuki N, Nagata K, et al. A novel computer-assisted measurement of the size of ossification in patients with ossification of the posterior longitudinal ligament in the cervical spine: development and reliability [in Japanese]. *Rinsho Seikeigeka* 2005;40:395–400.
13. Satomi K, Nishu Y, Kohno T, et al. Long-term follow-up studies of open-door expansive laminoplasty for cervical stenotic myelopathy. *Spine* 1994; 19:507–10.
14. Inoue H, Ohmori K, Ishida Y, et al. Long-term follow-up of suspension laminotomy for cervical compression myelopathy. *J Neurosurg* 1996;85: 817–23.
15. Ogawa Y, Toyama Y, Chiba K, et al. Long-term results of expansive open-door laminoplasty for ossification of the posterior longitudinal ligament of the cervical spine. *J Neurosurg* 2004;2:168–74.
16. Yonenobu K, Yamamoto T, Ono K. Laminoplasty for myelopathy: indications, results, outcomes and complications. In: Clark CR, ed. *The Cervical Spine,* 3rd ed. Philadelphia: Lippincott-Raven; 1998:849–64.
17. Matsunaga S, Sakou T, Taketomi E, et al. Clinical course of patients with ossification of the posterior longitudinal ligament: a minimum 10-year cohort study. *J Neurosurg (Spine 3)* 2004;100:245–8.

高齢関節リウマチ患者の頸椎病変に対する外科的治療*1

松永俊二*2　小宮節郎*3

はじめに

人口の高齢化が進む現代において脊椎病変を有する高齢者が増加している．以前は70歳以上の高齢者に対して脊椎の手術を施行することは例外的なものであり，手術の意義について言及されるようなことはほとんどなかった．しかし，最近は術後管理や手術方法の進歩に伴い，高齢者に対しても非高齢者と同様の手術が行われるようになった．わが国で脊椎手術を行っているほとんどすべての医療施設で全手術件数における高齢者脊椎手術の割合は年々増加している．この傾向は国民の健康寿命を延ばし医療費の削減を目指す国の政策と相まってますます加速していくように思われる．

多くの脊椎疾患のなかで関節リウマチによる脊椎疾患の手術を高齢患者に対して行う場合，留意すべき重要な点は基礎疾患である関節リウマチ自体の特殊性である．関節リウマチ患者の平均寿命は最近向上しているとはいえ，一般健常人に比べ明かに不良である[17,19,23]．また関節リウマチは全身性の疾患であり脊椎病変特に頻度の高い頸椎病変を呈する患者は大部分はステージが進行した患者である．脊椎手術を施行しても他の関節病変のため患者の健康寿命の改善につながることは少ない．周術期の合併症も関節リウマチ患者が高齢であればあるほど多いのも事実である．したがって現状では70歳以上の高齢関節リウマチ患者に対して脊椎手術を行う意義についてはまだ見解が統一されているとはいえない．関節リウマチ患者における脊椎病変で最も頻度が高くこれまで重要視されてきたのは，頸椎病変，特に上位頸椎病変である．本稿では高齢者関節リウマチ脊椎病変のなかでも頸椎病変について，手術適応や手術方法の選択および手術に伴う注意点について概説し，少ない症例ではあるが高齢者関節リウマチ頸椎手術の成績と意義について考察する．

Key words
環軸椎亜脱臼 (atlantoaxial subluxation)
高齢患者 (elderly patients)
後頭頸椎固定術 (occipitocervical fusion)

*1 Surgical Treatment for Cervical Lesions in the Elderly Patients with Rheumatoid Arthritis

*2 今給黎総合病院整形外科〔〒892-8502 鹿児島市下竜尾町4-16〕／Shunji MATSUNAGA：Department of Orthopaedic Surgery, Imakiire General Hospital
*3 鹿児島大学大学院運動機能修復学講座整形外科／Setsuro KOMIYA

0914-4412/07/¥400/論文/JCLS

日本における関節リウマチ頸椎手術の動向と高齢患者の位置づけ

関節リウマチによる頸椎病変に対する手術についてははこれまで多数報告がなされており，日本でも多くの学会でシンポジウムなどが組まれている．しかし，日本において関節リウマチの頸椎病変に対してどのくらいの数の手術が行われているかについての本格的な疫学的調査はこれまでほとんどなされていなかった．日本脊椎脊髄病学会の名のもとに行われた関節リウマチ頸椎手術全国アンケート調査によると，2001年の1年間に全国74施設で234名の関節リウマチ患者に対して頸椎手術が施行されている[15]．手術時年齢は33～85歳（平均64歳）であった．しかし，1施設あたり10例以上頸椎手術を施行している施設は3施設のみであり，他の施設は年間2～3例の症例しか頸椎手術を行っていない．この結果から判断すると，70歳以上の高齢者に対して頸椎手術を施行した症例はどの施設でも年間1例あるかない程度であると推定される．つまり現状ではまだ70歳以上の高齢関節リウマチ患者に対して頸椎手術を行うことは例外的であるといえよう．これは患者の平均寿命が一般人より短いため70歳以上の患者を治療する機会が少ないことと，術後の合併症などを危惧して手術に消極的になりがちであるという点が関係していると考えられる．

高齢者における手術の適応

関節リウマチの頸椎病変に対する手術の適応は，一般的には脊髄症状が認められる場合や神経根症状や頸部および後頭部痛が保存的治療で抑えられない場合である．脊髄症状の程度についてはRanawat分類[16]のclass IIIbでは手術を行っても脊髄症状の改善が得られなかったというCaseyら[3]の報告から，class IIIaまでに行うことを推奨する研究者が多い．Bodenら[2]は上位頸椎病変の患者で脊髄余裕空間（SAC）が10 mm以上に保たれている比較的軽度な病変での予防的な手術を推奨している．以上が関節リウマチの頸椎手術における一般的な手術適応であるが，70歳以上の高齢患者の場合はこの他にも留意すべき点があるように思う．まず患者の罹患している脊椎以外の全身病変を十分に把握する必要がある．関節病変とその重症度，過去に行われた手術の内容と術後の経過など，詳細な情報を得る必要がある．

患者をトータルで診療することの重要性は以前から強調されているが，専門化が進むほど自分の非専門領域の身体部位の病変への注意が散漫になりがちである．また関節リウマチは全身性疾患であり，整形外科領域以外の病変，特にアミロイドーシスの合併の検索は術後の生命予後に関係するため重要である[14]．以上のように関節リウマチ患者の全身状態を十分把握して手術に望まないと，予期しない合併症を生じて術後に不幸な結果を招いたり，手術は施行できても患者のQOL改善にはつながらず何のために手術を行ったかわからないような症例も出てくる．つまり高齢関節リウマチ患者の手術は患者の全身状態が良好であり手術の合併症の危険が少ない場合，そして手術によって患者のADLが改善しQOL改善につながる場合に行われるべきと考える．しばしば経験することであるが，すでに重度の身体機能障害のため介護施設などの入所している高齢関節リウマチ患者で頸椎病変が発見され手術を施行し無事退院しても，結局，元の介護施設に戻り適切なリハビリを受けることもなく身体運動機能の改善を達成できないことが多い．

清水らは関節リウマチの頸椎手術について別の意見を述べている[20,21]．関節リウマチによる頸椎病変を有する患者の中には呼吸・嚥下機能など生命維持に不可欠な機能も障害されているような重症例があり，このような症例では手術により呼吸機能の改善といった生命維持につながるだけで手術は意義があるとしている．このような特殊な高齢患者に対する手術は，手術を安全かつ的確に行える技量を持った医師が常勤し手術前後の管理が集中的に行える施設で行う必要がある．